

# High- $T_c$ ternary metal hydrides, $YKH_{12}$ and $LaKH_{12}$ , discovered by machine learning

Peng Song<sup>1</sup>, Zhufeng Hou<sup>2</sup>, Pedro Baptista de Castro<sup>3,4</sup>, Kousuke Nakano<sup>1,5</sup>, Kenta Hongo<sup>6</sup>, Yoshihiko Takano<sup>3,4</sup>, Ryo Maezono<sup>1</sup>

<sup>1</sup>*School of Information Science, JAIST, Asahidai 1-1, Nomi, Ishikawa 923-1292, Japan*

<sup>2</sup>*State Key Laboratory of Structural Chemistry, Fujian Institute of Research on the Structure of Matter, Chinese Academy of Sciences, Fuzhou 350002, China*

<sup>3</sup>*National Institute for Materials Science, 1-2-1 Sengen, Tsukuba, Ibaraki 305-0047, Japan*

<sup>4</sup>*University of Tsukuba, 1-1-1 Tennodai, Tsukuba, Ibaraki 305-8577, Japan*

<sup>5</sup>*International School for Advanced Studies (SISSA), Via Bonomea 265, 34136, Trieste, Italy*

<sup>6</sup>*Research Center for Advanced Computing Infrastructure, JAIST, Asahidai 1-1, Nomi, Ishikawa 923-1292, Japan*

(Dated: February 3, 2022)

The search for hydride compounds that exhibit high  $T_c$  superconductivity has been extensively studied. Within the range of binary hydride compounds, the studies have been developed well including data-driven searches as a topic of interest. Toward the search for the ternary systems, the number of possible combinations grows rapidly, and hence the power of data-driven search gets more prominent. In this study, we constructed various regression models to predict  $T_c$  for ternary hydride compounds and found the extreme gradient boosting (XGBoost) regression giving the best performance. The best performed regression predicts new promising candidates realizing higher  $T_c$ , for which we further identified their possible crystal structures. Confirming their lattice and thermodynamical stabilities, we finally predicted new ternary hydride superconductors,  $YKH_{12}$  [ $C2/m$  (No.12),  $T_c=143.2$  K at 240 GPa] and  $LaKH_{12}$  [ $R\bar{3}m$  (No.166),  $T_c=99.2$  K at 140 GPa] from first principles.

## INTRODUCTION

The compressed polyhydrides are good candidates for high  $T_c$  superconductor due to the high vibration frequencies provided by the hydrogen atoms, coupled with the introduction of other elements to get necessary pre-compression for the entire system to maintain its metallic and superconducting state even at lower pressure. The potential for high  $T_c$  has been confirmed by many theoretical and experimental studies. [1–5] The structure searching to get higher  $T_c$  for these compounds has been made mainly within binary compounds, and some of the synthesis have reported the achievement of high  $T_c$ , *e.g.*,  $LaH_{10}$  (260 K at 200 GPa), [6]  $YH_6$  (224 K at 166 GPa), [7] and  $TH_{10}$  (159 K at 174 GPa) [8] *etc.* Recent theoretical prediction of  $Li_2MgH_{16}$  (473 K at 250 GPa) and the experimental measurement of carbonaceous sulfur hydride (287 K at  $\sim 267$  GPa) indicate that multi component hydrides could have greater potential for higher  $T_c$  than binary ones. [9, 10] At present, about 10-20 ternary superconducting hydrides have been proposed, but a small part of them have been experimentally verified ending up with extremely low  $T_c$ . [9–29] According to 'Materials Project (MP) database', [30] the number of ternary compounds amounts around to five times larger than

that of binary compounds under ambient conditions, providing us with an exciting field of materials searching. For such problems with a wide search space, data-driven approaches get to be powerful over other methods. For cuprate and iron-based superconductors, their searchings by using machine learning approaches have been reported. [31–33] For the hydrides superconductor,  $RbH_{12}$ , neural networks have been applied. [34] We shall then employ machine learning techniques to explore ternary polyhydrides for higher  $T_c$ .

The compounds to be targeted were first narrowed down according to the following policy: The target ternary system is restricted within those composed as a combination of binary hydrides having higher  $T_c$  as reported. From binary hydrides that have been reported to be superconducting, [7, 21, 22, 25, 35–111] there can be about 2,800 possible combinations. Of these, except for those with very low  $T_c$ , we can narrow it down to about 1,800 types, and further, except for those with too high hydrogen content, to about 1,700 types. Among these, we limited our search to the Y and La systems which have tendency to achieve higher  $T_c$ , getting about 250 combinations of  $YMH_x$  and  $LaMH_x$  ( $M = Ca, K,$  and  $Na$ ). For these target compounds, a procedure for our virtual screening via machine-learning and high-throughput *ab*

*initio* calculations is as follows: (1) machine-learning search for the chemical compositions achieving higher  $T_c$ , (2) evolutionary crystal structure search for the candidate compositions, (3) stability check for the candidate structures, (4) *ab initio* predictions of  $T_c$  for the stable structures.

(1) For the composition search, as described in the “Method” section, we considered various regression models to predict  $T_c$  values of the ternary hydrides, which were learned with theoretically predicted data on  $T_c$  extracted from available literature. [7, 9, 11–15, 18–26, 35–122] Our descriptors entering the regression as input consist of 84 features such as chemical compositions, space group, and pressure-dependent electronic properties, where the composition descriptors were generated using the XenonPy software [123] and the pressure-dependent descriptors were computed by the VASP software [124–127]. We checked their prediction performance by using the cross validation and then the best performed model, *i.e.*, the extreme gradient boosting algorithm implemented in the XGBoost package, [128] was used for the high-throughput screening of the target ternary compounds. Our XGBoost model predicted ternary compositions,  $YKH_{12}$  and  $LaKH_{12}$ , to be candidates for achieving higher  $T_c$  at 200 GPa. (2) For the predicted chemical compositions, we further predicted their crystal structures by using an evolutionary algorithm for crystal structure search implemented in the USPEX code [129] coupled with *ab initio* geometry optimizations implemented in the VASP code. [124–127] (3) For the predicted crystal structures, as shown in Fig. 1, we evaluated their thermodynamical and structural stabilities by using convex hull method and *ab initio* phonon calculations. (4) Confirming the stabilities, we finally predicted that the ternary  $YKH_{12}$  and  $LaKH_{12}$  are promising candidates to achieve higher  $T_c$ . To the best of our knowledge, this is the first example of the ternary hydride superconductors realized by alkali earth metals ( $M=K$ , +2 valence) while other preceding studies with alkali metals ( $M = Ca, Mg$ , +1 valence).

## METHOD

Several ternary superconducting hydrides predicted theoretically so far, such as  $CaYH_{12}$ ,  $YSH_6$ , and  $CSH_7$ , [14, 25, 115] were proposed as a *composite* of two different binary hydrides possibly to form a compound under high pressure. Referring 102 published papers on superconducting hydrides, [7, 9, 11–15, 18–26, 35–122] we obtained 533 superconducting data, including 181 high- $T_c$  hydrides ( $T_c$  higher than liquid nitrogen). Additionally, we collected 150 kinds of binary compounds. Excluding those with very low  $T_c$  ( $T_c < 40$  K, McMillan Limit), 81 kinds were left. They can form 2,867 ternary combinations excluding the overlap of chemical compositions. Moreover, we excluded those with extremely higher hydrogen concentration, making  $x \leq 16$  for  $AMH_x$ , [9] thereby obtaining 2,366 possible compounds. To make the search space more compact, we selected the candidates only

for those with  $A=La$  and  $Y$  because La- and Y-based materials have well been verified as having higher  $T_c$  by not only theoretical predictions, but also experimental observations [6, 7]. Resultant candidates,  $YMH_x$  and  $LaMH_x$ , then amount to 238 compounds, which are input compounds entering the regression.

It is difficult to obtain all the structural data from the above pool of published articles. It is rather practical to use chemical compositions as the direct descriptor. In the preceding studies, [130–134] it has been found that  $T_c$  correlates well with (i) space group, [6, 135] (ii) density of states (DOS) at the Fermi level,  $D(E_F)$ , as a measure of the applied pressure, [73, 76, 101, 131, 136] as well as (iii) the chemical composition. [132, 137] By the procedures explained below, we finally set up total 84 descriptors corresponding to the above three features: For (i) [space group], we took the number index for the space group (*e.g.*, No.166 for  $R\bar{3}m$ ) as the descriptor. For (ii) [pressure], we used the scheme taken in the preceding studies, [32, 138] where the descriptors were composed as weighted averages over the quantities for pristine materials composed of each of elements in a compound (averaging weight is based on the composition ratio). The quantities were evaluated for the structure of each pristine material taken from the Materials Project [30] by using VASP [124–127] to get DOS at several values of pressure (detailed computational conditions were provided in S.I. (§)). For the weighted averaging, we took the same manner as in XenonPy. [123] The procedure provides total 56 descriptors for (ii) at this stage. For (iii) [chemical composition], we used a XenonPy utility [123] that generates many possible descriptors, from which we picked up 290 descriptors at the first stage.

For total 347 descriptors [290 (iii/Chemical composition) + 56 (ii/pressure dependent DOS) + 1 (i/space group number)], we truncated them to avoid overfitting by excluding those with comparably weaker correlation with  $T_c$ . The truncation can be performed during the random-forest regressions by monitoring the correlation using the scikit-learn library [139] (with six trees for this purpose), finally getting total 84 truncated descriptors [70 (iii/Chemical composition) + 13 (ii/pressure dependent DOS) + 1 (space group number)] as listed in S.I. (§).

The above constructed descriptors were thoroughly incorporated into four linear Ridge (RD), [140] Bayesian Ridge (RD), [141] LASSO (LS), [140, 142–144] and Elastic Net (EN) [140, 145]) and three nonlinear Decision-Tree (DT) [140], Random Forest (RF) [140, 146, 147], and Extreme Gradient Boosting (XGBoost) [128, 140]) regressors to predict  $T_c$  for the target compositions (see Table I); the (maximum) depths of decision tree for DT, RF, and XGBoost were set to be 21, 16, and 7, respectively. To construct the regressors, 533 data [7, 9, 11–15, 18–26, 35–122] are randomly divided into training and test data with with the ratio of 80:20. Hyperparameters in the models were chosen through the Bayesian optimization technique implemented in the Hy-

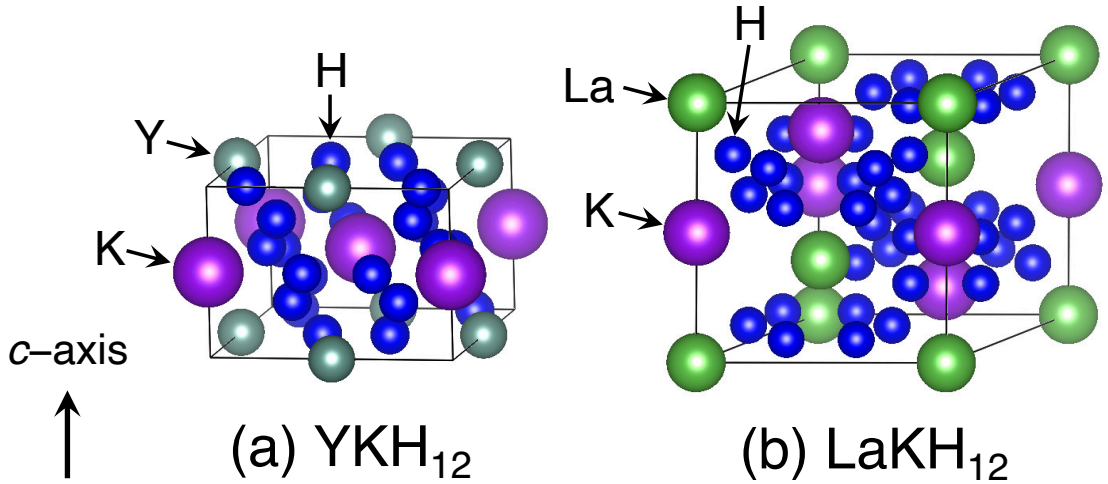


FIG. 1. Predicted structures for (a)  $YKH_{12}$  with  $C2/m$  (No.12), and (b)  $LaKH_{12}$  with  $R\bar{3}m$  (No.166), by the crystal structures search using USPEX.

TABLE I. Comparison of several regression models in terms of  $R^2$ , MAE (Mean Absolute Error), and RMSE (Root Mean Squared Error) for the test dataset. Each abbreviation means 'RD' (Ridge), 'BR' (Bayesian Ridge), 'LS' (Lasso), 'EN' (Elastic Net), 'DT' (Decision Tree), 'RF' (Random Forest), and 'XGB' (Extreme Gradient Boosting).

	Linear regression				Nonlinear regression		
	RD	BR	LS	EN	DT	RF	XGB
$R^2$	0.244	0.249	0.403	0.460	0.732	0.842	0.877
MAE	34.66	37.57	34.06	32.24	18.58	16.34	13.53
RMSE	50.34	50.17	44.75	42.56	29.96	23.01	20.29

perOpt software package [148] to minimize the  $R^2$  5-fold cross-validation score. Model performance was judged from  $R^2$ , MAE (Mean Absolute Error), and RMSE (Root Mean Squared Error) as given in Table I. Among the above regressors, we found the XGBoost exhibiting the best performance for the test data, *i.e.*, the lowest RMSE,  $\Delta T^{\text{RMSE}} \sim 20$  K. Thus, the XGBoost was chosen as our machine learning model for  $T_c$ -prediction used in the successive high-throughput virtual screening of the ternary compositions.

Once a trained regression is available, it can immediately predict  $T_c$  even for the chemical compositions with unknown  $T_c$  by putting corresponding descriptors as the input for the regression. Since we do not know their crystal structures in advance for the predictions, we have to assume their space groups in order to complete input descriptors. Looking over the existing data, we found that a space group,  $R\bar{3}m$  (No.166), often gives higher  $T_c$  for binary compounds, so we adopted it as a trial. The trial setting was proved to be a fair choice by further verifications (crystal structural predictions and *ab ini-*

*titio* estimations) in a consistent manner as explained later. On the assumption of space group, we predicted  $T_c$  for several choices of  $XMH_x$  ( $X=Y$  and La). For the candidate chemical composition giving higher  $T_c$ , we further predict their crystal structure by using the USPEX code [129] combined with *ab initio* kernel by VASP. [124–127] It randomly generates the 400 structures among from monomer upto tetramer of  $AKH_{12}$  ( $A = \text{La}$  or  $\text{Y}$ ) as an 'initial generation' for the generic algorithm. Each generation evolves 100 structures according to 40% heredity, 40% random, 10% softmutation, and 10% transmutation. A promising candidate structure is identified when no further evolution occurs for more than 10 generations. The candidate is then subject to further *ab initio* geometrical optimizations by using the Perdew-Burke-Ernzerhof (GGA-PBE) functional for the exchange-correlation functional. [149] We performed the procedure at the pressure of 100 GPa, 200 GPa, and 300 GPa, to get each optimized structure.

For the predicted crystal structures, we evaluated the structural stability by phonon calculations and thermodynamic stability by the convex hull method. For the phonon evaluations, we used the PhonoPy package [150] combined with *ab initio* kernel by VASP. [124–127] Convex hull evaluations were made by using a utility implemented in USPEX. [129] By the *ab initio* phonon calculations, we finally estimated  $T_c$  based on the Allen-Dynes formalism, [151, 152] to be compared with our data-driven predictions by the regression for verification. Detailed computational conditions for the phonon calculations are given in S.I. (§).

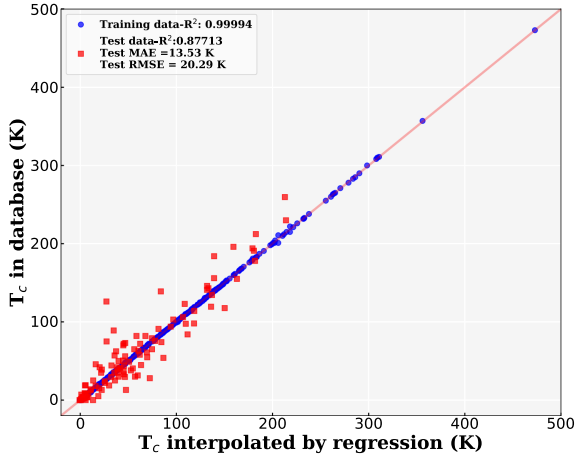


FIG. 2. Model performance. Comparison between  $T_c$  in database and that interpolated by regression, proving the performance of our XGBoost regression model. Total 533 data are randomly divided into 426 training data (80%) and 107 test data (20%).

## RESULTS AND DISCUSSION

As we mentioned in the previous section (see Table I), the XGBoost regressor is the best performed machine learning model. Fig. 2 shows the performance of our XGBoost model. Its  $R^2$  values are 0.99 and 0.87 for 426 training and 107 test data, respectively, indicating our regressor is slightly overfitted. But it exhibits a better performance than the other models, especially the linear regressions. Looking at RMSE, the XGBoost value was about 20 K. This cannot matter for our purpose of the virtual screening if we keep in mind that our machine-learning prediction of  $T_c$  could deviate from the corresponding *ab initio* prediction by  $\pm 20$  K with a 68% confidence level.

Getting a good trained regression, we should be able to perform the virtual screening via the machine learning to search composite candidates with unknown  $T_c$  for high- $T_c$  compounds. We applied the XGBoost regression to predict  $T_c$  for 238  $AMH_x$ -type composites, as we mentioned. 11.7% of the total composites were found to be of  $AMH_{12}$ -type (*i.e.*  $x = 12$ ) having higher  $T_c$ . We then narrowed down the candidates within the  $AMH_{12}$ -type candidates to get 28 compounds. Among the 28 candidates, we found that the composition  $YKH_{12}$  achieves the highest value of  $T_c$ , followed by  $LaKH_{12}$  as the second highest one, as shown in Table II. For reference, the remaining  $T_c$  values are given in the supporting information (Table VI).

For the predicted compositions to achieve higher  $T_c$ ,  $YKH_{12}$  and  $LaKH_{12}$ , we performed further predictions for their crystal structures by using USPEX. [129] The predicted

TABLE II. Comparison of the  $T_c$  predictions between the *ab initio* DFT and the XGBoost regression.

Composite	Predicted $T_c$ [K]	
	Regression	<i>Ab initio</i>
$YKH_{12}$	168.9	143.2
$LaKH_{12}$	162.8	99.2

structures are shown in Fig. 1. The space group  $R\bar{3}m$ (No.166) concluded for  $LaKH_{12}$  is consistent with our initial guess of the structural symmetry as the input descriptor for our regression.

To strengthen the reality of predictions, it is indispensable to estimate the stability of the predicted structures. The thermal stability of the structure is confirmed by comparing a pressure dependence of relative formation enthalpy within the USPEX calculations as shown in Fig. 3. From the analysis, we can identify the pressure range where the structures can stably exist. Under the pressure range, we performed *ab initio* phonon calculations to examine the lattice stabilities. [151, 152] As shown in Fig. 4, any imaginary modes do not appear ensuring the lattice stability for these structures at the pressure.

For  $YKH_{12}$  (at 240 GPa) and  $LaKH_{12}$  (at 160 GPa), we further evaluated their electron-phonon couplings and then estimated their  $T_c$  values based on the Allen-Dynes formalism, [151, 152] which are listed in Table II. The machine-learning predicted values overestimate *ab initio* ones by  $\sim 20$ K and  $\sim 60$ K for  $YKH_{12}$  and  $LaKH_{12}$ , respectively. These overestimates lie within almost RMSE and three-times RMSE, respectively, which may be thought of as being allowable, judging from our XGBoost performance.

## CONCLUSION

We performed a data-driven materials searching for ternary hydrides superconductors within the range of  $AMH_{12}$  ( $A=La, Y$ ) composition. The regression over 533 existing superconductors was constructed by the random forest method using 84 descriptors characterizing chemical composition, space group, and pressure. Using the regression, we estimated  $T_c$  over 239 compositions to get the prediction of higher  $T_c$  achieved by the choice of  $M=K$ ,  $YKH_{12}$  and  $LaKH_{12}$ . For the predicted compositions, we performed evolutionary structure search to get their crystal structures. For the structures, we confirmed their structural stabilities by using *ab initio* phonon calculations as well as getting  $T_c$  estimated by Allen-Dynes formula. We finally predicted two new ternary hydrides superconductors,  $YKH_{12}$  [ $C2/m$  (No.12),  $T_c=143.2$  K at 240 GPa] and  $LaKH_{12}$  [ $R\bar{3}m$  (No.166),  $T_c=99.2$  K at 140 GPa].

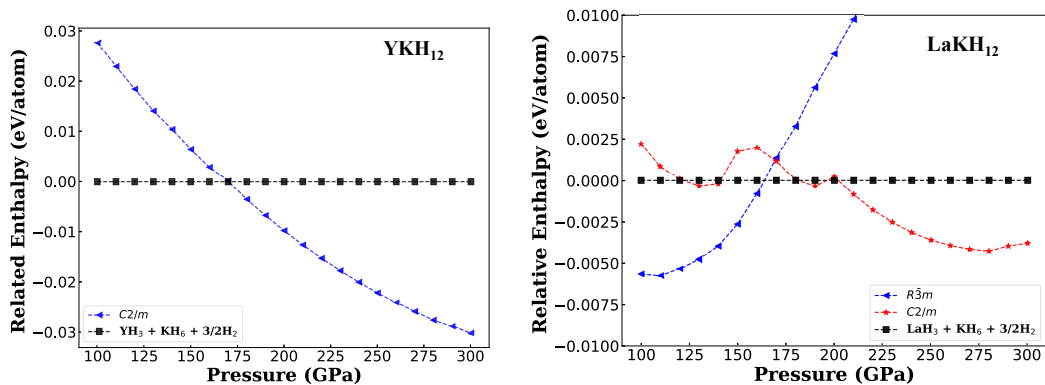


FIG. 3. Relative enthalpies for (a)  $\text{YKH}_{12}$  and (b)  $\text{LaKH}_{12}$ , showing the pressure range where the compounds are stable.

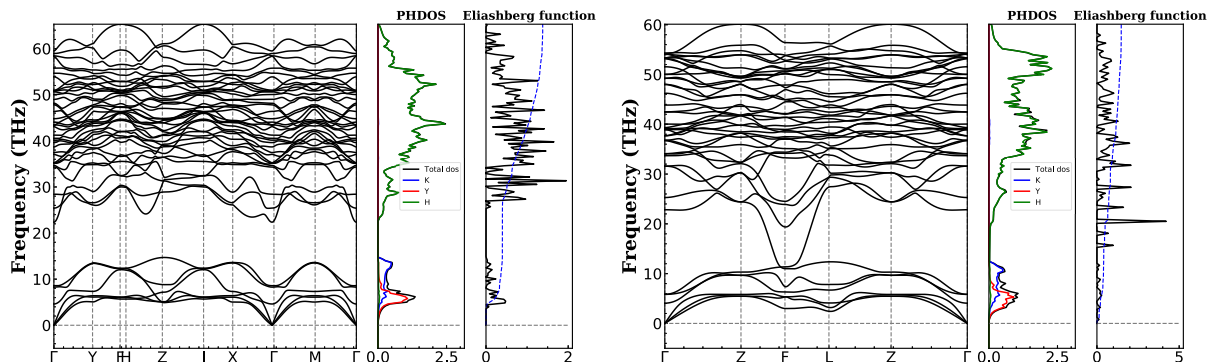


FIG. 4. Phonon dispersions, phonon DOS, and Eliashberg functions for (a)  $\text{YKH}_{12}$  at 200 GPa and (b)  $\text{LaKH}_{12}$  at 160 GPa. No imaginary frequency appears ensuring the lattice stability for each compound.

## ACKNOWLEDGMENTS

The computations in this work have been performed using the facilities of Research Center for Advanced Computing Infrastructure (RCACI) at JAIST. K.H. is grateful for financial support from the HPCI System Research Project (Project ID: hp190169) and MEXT-KAKENHI (JP16H06439, JP17K17762, JP19K05029, and JP19H05169). R.M. is grateful for financial supports from MEXT-KAKENHI (19H04692 and 16KK0097), FLAGSHIP2020 (project nos. hp1 90169 and hp190167 at K-computer), Toyota Motor Corporation, I-O DATA Foundation, the Air Force Office of Scientific Research (AFOSR-AOARD/FA2386-17-1-4049;FA2386-19-1-4015), and JSPS Bilateral Joint Projects (with India DST).

- 
- [1] N. Ashcroft, Physical Review Letters **92**, 187002 (2004).  
 [2] N. W. Ashcroft, Physical Review Letters **21**, 1748 (1968).  
 [3] M. Erements, I. Trojan, S. Medvedev, J. Tse, and Y. Yao, Science **319**, 1506 (2008).

- [4] A. Drozdov, M. Erements, I. Troyan, V. Ksenofontov, and S. I. Shylin, Nature **525**, 73 (2015).  
 [5] D. Szczęśniak and T. Zemła, Superconductor Science and Technology **28**, 085018 (2015).  
 [6] M. Somayazulu, M. Ahart, A. K. Mishra, Z. M. Geballe, M. Baldini, Y. Meng, V. V. Struzhkin, and R. J. Hemley, Physical review letters **122**, 027001 (2019).  
 [7] I. A. Troyan, D. V. Semenok, A. G. Kvashnin, A. V. Sadakov, O. A. Sobolevskiy, V. M. Pudalov, A. G. Ivanova, V. B. Prakapenka, E. Greenberg, A. G. Gavriliuk, *et al.*, arXiv preprint arXiv:1908.01534 (2020).  
 [8] D. V. Semenok, I. A. Kruglov, I. A. Savkin, A. G. Kvashnin, and A. R. Oganov, Current Opinion in Solid State and Materials Science , 100808 (2020).  
 [9] Y. Sun, J. Lv, Y. Xie, H. Liu, and Y. Ma, Physical review letters **123**, 097001 (2019).  
 [10] E. Snider, N. Dasenbrock-Gammon, R. McBride, M. Debesai, H. Vindana, K. Vencatasamy, K. V. Lawler, A. Salamat, and R. P. Dias, Nature **586**, 373 (2020).  
 [11] Y. Ma, D. Duan, Z. Shao, H. Yu, H. Liu, F. Tian, X. Huang, D. Li, B. Liu, and T. Cui, Physical Review B **96**, 144518 (2017).  
 [12] Y. Ma, D. Duan, Z. Shao, D. Li, L. Wang, H. Yu, F. Tian, H. Xie, B. Liu, and T. Cui, Physical Chemistry Chemical Physics **19**, 27406 (2017).

- [13] D. Li, Y. Liu, F.-B. Tian, S.-L. Wei, Z. Liu, D.-F. Duan, B.-B. Liu, and T. Cui, *Frontiers of Physics* **13**, 137107 (2018).
- [14] X. Liang, S. Zhao, C. Shao, A. Bergara, H. Liu, L. Wang, R. Sun, Y. Zhang, Y. Gao, Z. Zhao, *et al.*, *Physical Review B* **100**, 184502 (2019).
- [15] M. Rahm, R. Hoffmann, and N. Ashcroft, *Journal of the American Chemical Society* **139**, 8740 (2017).
- [16] X. Liang, A. Bergara, L. Wang, B. Wen, Z. Zhao, X.-F. Zhou, J. He, G. Gao, and Y. Tian, *Physical Review B* **99**, 100505 (2019).
- [17] Y. K. Wei, L. Q. Jia, Y. Y. Fang, L. J. Wang, Z. X. Qian, J. N. Yuan, G. Selvaraj, G. F. Ji, and D. Q. Wei, *International Journal of Quantum Chemistry*, e26459 (2020).
- [18] H. Xie, D. Duan, Z. Shao, H. Song, Y. Wang, X. Xiao, D. Li, F. Tian, B. Liu, and T. Cui, *Journal of Physics: Condensed Matter* **31**, 245404 (2019).
- [19] C. Kokail, W. von der Linden, and L. Boeri, *Physical Review Materials* **1**, 074803 (2017).
- [20] Z. Shao, D. Duan, Y. Ma, H. Yu, H. Song, H. Xie, D. Li, F. Tian, B. Liu, and T. Cui, *npj Computational Materials* **5**, 1 (2019).
- [21] J. Zhang, J. M. McMahon, A. R. Oganov, X. Li, X. Dong, H. Dong, and S. Wang, *Physical Review B* **101**, 134108 (2020).
- [22] P. Zhang, Y. Sun, X. Li, J. Lv, and H. Liu, *Physical Review B* **102**, 184103 (2020).
- [23] S. Di Cataldo, W. von der Linden, and L. Boeri, *Physical Review B* **102**, 014516 (2020).
- [24] X. Guo, R.-L. Wang, H.-L. Chen, W.-C. Lu, K. Ho, and C. Wang, *Physics Letters A* **384**, 126189 (2020).
- [25] W. Cui, T. Bi, J. Shi, Y. Li, H. Liu, E. Zurek, and R. J. Hemley, *Physical Review B* **101**, 134504 (2020).
- [26] H.-Y. Lv, S.-Y. Zhang, M.-H. Li, Y.-L. Hai, N. Lu, W.-J. Li, and G.-H. Zhong, *Physical Chemistry Chemical Physics* **22**, 1069 (2020).
- [27] Y. Yan, T. Bi, N. Geng, X. Wang, and E. Zurek, *The Journal of Physical Chemistry Letters* **11**, 9629 (2020).
- [28] T. Muramatsu, W. K. Wanene, M. Somayazulu, E. Vinitzky, D. Chandra, T. A. Strobel, V. V. Struzhkin, and R. J. Hemley, *The Journal of Physical Chemistry C* **119**, 18007 (2015).
- [29] D. Meng, M. Sakata, K. Shimizu, Y. Iijima, H. Saitoh, T. Sato, S. Takagi, and S.-i. Orimo, *Physical Review B* **99**, 024508 (2019).
- [30] A. Jain, S. P. Ong, G. Hautier, W. Chen, W. D. Richards, S. Dacek, S. Cholia, D. Gunter, D. Skinner, G. Ceder, *et al.*, *Apl Materials* **1**, 011002 (2013).
- [31] V. Stanev, C. Oses, A. G. Kusne, E. Rodriguez, J. Paglione, S. Curtarolo, and I. Takeuchi, *npj Computational Materials* **4**, 1 (2018).
- [32] K. Matsumoto and T. Horide, *Applied Physics Express* **12**, 073003 (2019).
- [33] B. Meredig, E. Antono, C. Church, M. Hutchinson, J. Ling, S. Paradiso, B. Blaiszik, I. Foster, B. Gibbons, J. Hattrick-Simpers, *et al.*, *Molecular Systems Design & Engineering* **3**, 819 (2018).
- [34] M. J. Hutcheon, A. M. Shipley, and R. J. Needs, *Physical Review B* **101**, 144505 (2020).
- [35] X.-J. Chen, J.-L. Wang, V. V. Struzhkin, H.-k. Mao, R. J. Hemley, and H.-Q. Lin, *Physical review letters* **101**, 077002 (2008).
- [36] D. Y. Kim, R. H. Scheicher, and R. Ahuja, *Physical review letters* **103**, 077002 (2009).
- [37] S. T. John, Z. Song, Y. Yao, J. S. Smith, S. Desgreniers, and D. D. Klug, *Solid state communications* **149**, 1944 (2009).
- [38] X. Jin, X. Meng, Z. He, Y. Ma, B. Liu, T. Cui, G. Zou, and H.-k. Mao, *Proceedings of the National Academy of Sciences* **107**, 9969 (2010).
- [39] Y. Li, G. Gao, Y. Xie, Y. Ma, T. Cui, and G. Zou, *Proceedings of the National Academy of Sciences* **107**, 15708 (2010).
- [40] G. Gao, A. R. Oganov, P. Li, Z. Li, H. Wang, T. Cui, Y. Ma, A. Bergara, A. O. Lyakhov, T. Itaka, *et al.*, *Proceedings of the National Academy of Sciences* **107**, 1317 (2010).
- [41] D. Duan, F. Tian, Z. He, X. Meng, L. Wang, C. Chen, X. Zhao, B. Liu, and T. Cui, *The Journal of chemical physics* **133**, 074509 (2010).
- [42] G. Gao, H. Wang, A. Bergara, Y. Li, G. Liu, and Y. Ma, *Physical Review B* **84**, 064118 (2011).
- [43] D. Y. Kim, R. H. Scheicher, C. J. Pickard, R. Needs, and R. Ahuja, *Physical review letters* **107**, 117002 (2011).
- [44] K. Abe and N. Ashcroft, *Physical Review B* **84**, 104118 (2011).
- [45] G. Zhong, C. Zhang, X. Chen, Y. Li, R. Zhang, and H. Lin, *The Journal of Physical Chemistry C* **116**, 5225 (2012).
- [46] C. Zhang, X.-J. Chen, and H.-Q. Lin, *Journal of Physics: Condensed Matter* **24**, 035701 (2011).
- [47] D. Zhou, X. Jin, X. Meng, G. Bao, Y. Ma, B. Liu, and T. Cui, *Physical Review B* **86**, 014118 (2012).
- [48] G. Gao, R. Hoffmann, N. W. Ashcroft, H. Liu, A. Bergara, and Y. Ma, *Physical Review B* **88**, 184104 (2013).
- [49] K. Abe and N. Ashcroft, *Physical Review B* **88**, 174110 (2013).
- [50] J. Hooper, B. Altintas, A. Shamp, and E. Zurek, *The Journal of Physical Chemistry C* **117**, 2982 (2013).
- [51] D. C. Lonie, J. Hooper, B. Altintas, and E. Zurek, *Physical Review B* **87**, 054107 (2013).
- [52] C.-H. Hu, A. R. Oganov, Q. Zhu, G.-R. Qian, G. Frapper, A. O. Lyakhov, and H.-Y. Zhou, *Physical review letters* **110**, 165504 (2013).
- [53] Y. Xie, Q. Li, A. R. Oganov, and H. Wang, *Acta Crystallographica Section C: Structural Chemistry* **70**, 104 (2014).
- [54] S. Yu, Q. Zeng, A. R. Oganov, C. Hu, G. Frapper, and L. Zhang, *AIP Advances* **4**, 107118 (2014).
- [55] Y. Li, J. Hao, H. Liu, Y. Li, and Y. Ma, *The Journal of chemical physics* **140**, 174712 (2014).
- [56] Z. Wang, Y. Yao, L. Zhu, H. Liu, T. Itaka, H. Wang, and Y. Ma, *The Journal of chemical physics* **140**, 124707 (2014).
- [57] C. Chen, F. Tian, D. Duan, K. Bao, X. Jin, B. Liu, and T. Cui, *The Journal of Chemical Physics* **140**, 114703 (2014).
- [58] D. Duan, Y. Liu, F. Tian, D. Li, X. Huang, Z. Zhao, H. Yu, B. Liu, W. Tian, and T. Cui, *Scientific reports* **4**, 6968 (2014).
- [59] X. Yan, Y. Chen, X. Kuang, and S. Xiang, *The Journal of chemical physics* **143**, 124310 (2015).
- [60] P. Hou, X. Zhao, F. Tian, D. Li, D. Duan, Z. Zhao, B. Chu, B. Liu, and T. Cui, *RSC advances* **5**, 5096 (2015).
- [61] D. Duan, F. Tian, Y. Liu, X. Huang, D. Li, H. Yu, Y. Ma, B. Liu, and T. Cui, *Physical Chemistry Chemical Physics* **17**, 32335 (2015).
- [62] H. Zhang, X. Jin, Y. Lv, Q. Zhuang, Y. Liu, Q. Lv, K. Bao, D. Li, B. Liu, and T. Cui, *Scientific reports* **5**, 8845 (2015).
- [63] Y. Liu, X. Huang, D. Duan, F. Tian, H. Liu, D. Li, Z. Zhao, X. Sha, H. Yu, H. Zhang, *et al.*, *Scientific reports* **5**, 11381 (2015).
- [64] A. Shamp and E. Zurek, *The Journal of Physical Chemistry Letters* **6**, 4067 (2015).
- [65] Y. Liu, D. Duan, X. Huang, F. Tian, D. Li, X. Sha, C. Wang, H. Zhang, T. Yang, B. Liu, *et al.*, *The Journal of Physical Chemistry C* **119**, 15905 (2015).



- [66] C. Chen, Y. Xu, X. Sun, and S. Wang, *The Journal of Physical Chemistry C* **119**, 17039 (2015).
- [67] X. Feng, J. Zhang, G. Gao, H. Liu, and H. Wang, *RSC advances* **5**, 59292 (2015).
- [68] H. Zhang, X. Jin, Y. Lv, Q. Zhuang, Q. Lv, Y. Liu, K. Bao, D. Li, B. Liu, and T. Cui, *Physical Chemistry Chemical Physics* **17**, 27630 (2015).
- [69] Y. Liu, D. Duan, F. Tian, H. Liu, C. Wang, X. Huang, D. Li, Y. Ma, B. Liu, and T. Cui, *Inorganic chemistry* **54**, 9924 (2015).
- [70] S. Yu, X. Jia, G. Frapper, D. Li, A. R. Oganov, Q. Zeng, and L. Zhang, *Scientific reports* **5**, 17764 (2015).
- [71] Y. Cheng, C. Zhang, T. Wang, G. Zhong, C. Yang, X.-J. Chen, and H.-Q. Lin, *Scientific reports* **5**, 16475 (2015).
- [72] S. Zhang, Y. Wang, J. Zhang, H. Liu, X. Zhong, H.-F. Song, G. Yang, L. Zhang, and Y. Ma, *Scientific reports* **5**, 1 (2015).
- [73] I. Errea, M. Calandra, C. J. Pickard, J. Nelson, R. J. Needs, Y. Li, H. Liu, Y. Zhang, Y. Ma, and F. Mauri, *Physical Review Letters* **114**, 157004 (2015).
- [74] T. Ishikawa, A. Nakanishi, K. Shimizu, H. Katayama-Yoshida, T. Oda, and N. Suzuki, *Scientific reports* **6**, 23160 (2016).
- [75] M. M. D. Esfahani, Z. Wang, A. R. Oganov, H. Dong, Q. Zhu, S. Wang, M. S. Rikitin, and X.-F. Zhou, *Scientific reports* **6**, 22873 (2016).
- [76] Y. Fu, X. Du, L. Zhang, F. Peng, M. Zhang, C. J. Pickard, R. J. Needs, D. J. Singh, W. Zheng, and Y. Ma, *Chemistry of Materials* **28**, 1746 (2016).
- [77] A. Shamp, T. Terpstra, T. Bi, Z. Falls, P. Avery, and E. Zurek, *Journal of the American Chemical Society* **138**, 1884 (2016).
- [78] Y. Liu, D. Duan, F. Tian, C. Wang, Y. Ma, D. Li, X. Huang, B. Liu, and T. Cui, *Physical Chemistry Chemical Physics* **18**, 1516 (2016).
- [79] X. Li, H. Liu, and F. Peng, *Physical Chemistry Chemical Physics* **18**, 28791 (2016).
- [80] X. Zhong, H. Wang, J. Zhang, H. Liu, S. Zhang, H.-F. Song, G. Yang, L. Zhang, and Y. Ma, *Physical Review Letters* **116**, 057002 (2016).
- [81] Y. Li, L. Wang, H. Liu, Y. Zhang, J. Hao, C. J. Pickard, J. R. Nelson, R. J. Needs, W. Li, Y. Huang, *et al.*, *Physical Review B* **93**, 020103 (2016).
- [82] X. Li and F. Peng, *Inorganic chemistry* **56**, 13759 (2017).
- [83] Q. Zhuang, X. Jin, T. Cui, Y. Ma, Q. Lv, Y. Li, H. Zhang, X. Meng, and K. Bao, *Inorganic chemistry* **56**, 3901 (2017).
- [84] H. Liu, I. I. Naumov, R. Hoffmann, N. Ashcroft, and R. J. Hemley, *Proceedings of the National Academy of Sciences* **114**, 6990 (2017).
- [85] Q. Zeng, S. Yu, D. Li, A. R. Oganov, and G. Frapper, *Physical Chemistry Chemical Physics* **19**, 8236 (2017).
- [86] T. Ishikawa, A. Nakanishi, K. Shimizu, and T. Oda, *Journal of the Physical Society of Japan* **86**, 124711 (2017).
- [87] X.-F. Li, Z.-Y. Hu, and B. Huang, *Physical Chemistry Chemical Physics* **19**, 3538 (2017).
- [88] F. Peng, Y. Sun, C. J. Pickard, R. J. Needs, Q. Wu, and Y. Ma, *Physical review letters* **119**, 107001 (2017).
- [89] M. M. D. Esfahani, A. R. Oganov, H. Niu, and J. Zhang, *Physical Review B* **95**, 134506 (2017).
- [90] A. Majumdar, S. T. John, M. Wu, and Y. Yao, *Physical Review B* **96**, 201107 (2017).
- [91] N. Zarifi, T. Bi, H. Liu, and E. Zurek, *The Journal of Physical Chemistry C* **122**, 24262 (2018).
- [92] D. V. Semenov, A. G. Kvashnin, I. A. Kruglov, and A. R. Oganov, *The journal of physical chemistry letters* **9**, 1920 (2018).
- [93] X. Ye, N. Zarifi, E. Zurek, R. Hoffmann, and N. Ashcroft, *The Journal of Physical Chemistry C* **122**, 6298 (2018).
- [94] A. G. Kvashnin, D. V. Semenov, I. A. Kruglov, I. A. Wrona, and A. R. Oganov, *ACS applied materials & interfaces* **10**, 43809 (2018).
- [95] A. P. Durajski and R. Szcześniak, *The Journal of chemical physics* **149**, 074101 (2018).
- [96] S. Zheng, S. Zhang, Y. Sun, J. Zhang, J. Lin, G. Yang, and A. Bergara, *Frontiers in Physics* **6**, 101 (2018).
- [97] K. Abe, *Physical Review B* **98**, 134103 (2018).
- [98] Q. Zhuang, X. Jin, T. Cui, D. Zhang, Y. Li, X. Li, K. Bao, and B. Liu, *Physical Review B* **98**, 024514 (2018).
- [99] A. G. Kvashnin, I. A. Kruglov, D. V. Semenov, and A. R. Oganov, *The Journal of Physical Chemistry C* **122**, 4731 (2018).
- [100] J. Wu, L.-Z. Zhao, H.-L. Chen, D. Wang, J.-Y. Chen, X. Guo, Q.-J. Zang, and W.-C. Lu, *physica status solidi (b)* **255**, 1800224 (2018).
- [101] C. Heil, S. Di Cataldo, G. B. Bachelet, and L. Boeri, *Physical Review B* **99**, 220502 (2019).
- [102] X. Li, X. Huang, D. Duan, C. J. Pickard, D. Zhou, H. Xie, Q. Zhuang, Y. Huang, Q. Zhou, B. Liu, *et al.*, *Nature communications* **10**, 1 (2019).
- [103] Y. Yuan, Y. Li, G. Fang, G. Liu, C. Pei, X. Li, H. Zheng, K. Yang, and L. Wang, *National Science Review* **6**, 524 (2019).
- [104] D. Wang, H. Zhang, H.-L. Chen, J. Wu, Q.-J. Zang, and W.-C. Lu, *Physics Letters A* **383**, 774 (2019).
- [105] W.-H. Yang, W.-C. Lu, S.-D. Li, X.-Y. Xue, Q.-J. Zang, K.-M. Ho, and C.-Z. Wang, *Physical Chemistry Chemical Physics* **21**, 5466 (2019).
- [106] R. Xi, Y. Jing, J. Li, Y. Deng, X. Cao, and G. Yang, *The Journal of Physical Chemistry C* **123**, 24243 (2019).
- [107] K. Abe, *Physical Review B* **100**, 174105 (2019).
- [108] H. Xie, W. Zhang, D. Duan, X. Huang, Y. Huang, H. Song, X. Feng, Y. Yao, C. J. Pickard, and T. Cui, *The Journal of Physical Chemistry Letters* **11**, 646 (2020).
- [109] Y. Ma, D. Duan, D. Li, Y. Liu, F. Tian, H. Yu, C. Xu, Z. Shao, B. Liu, and T. Cui, *arXiv preprint arXiv:1511.05291* (2015).
- [110] H. Li, X. Li, H. Wang, G. Liu, Y. Li, and H. Liu, *New Journal of Physics* **21**, 123009 (2019).
- [111] S. Kanagaprabha and R. Rajeswarapalanichamy, *Journal of Materials Science Research and Reviews* , 1 (2018).
- [112] S. Zhang, L. Zhu, H. Liu, and G. Yang, *Inorganic Chemistry* **55**, 11434 (2016).
- [113] B. Liu, W. Cui, J. Shi, L. Zhu, J. Chen, S. Lin, R. Su, J. Ma, K. Yang, M. Xu, *et al.*, *Physical Review B* **98**, 174101 (2018).
- [114] A. Nakanishi, T. Ishikawa, and K. Shimizu, *Journal of the Physical Society of Japan* **87**, 124711 (2018).
- [115] X. Liang, A. Bergara, L. Wang, B. Wen, Z. Zhao, X.-F. Zhou, J. He, G. Gao, and Y. Tian, *Physical Review B* **99**, 100505 (2019).
- [116] K. Grishakov, N. Degtyarenko, and E. Mazur, *Journal of Experimental and Theoretical Physics* **128**, 105 (2019).
- [117] J. Chen, X. Xue, H. Chen, H. Liu, Q. Zang, and W. Lu, *The Journal of Physical Chemistry C* **123**, 28008 (2019).
- [118] M. Amsler, *Physical Review B* **99**, 060102 (2019).
- [119] X. Du, S. Zhang, J. Lin, X. Zhang, A. Bergara, and G. Yang, *Physical Review B* **100**, 134110 (2019).
- [120] X. Li, Y. Xie, Y. Sun, P. Huang, H. Liu, C. Chen, and Y. Ma, *The Journal of Physical Chemistry Letters* **11**, 935 (2020).
- [121] L. Hao, Z. Yuan, X. Guo, Y. Zhang, K. Luo, Y. Gao, F. Ling, X. Chen, Z. Zhao, and D. Yu, *Physics Letters A* , 126525 (2020).

- [122] L. Hao, Z. Yuan, X. Guo, Y. Zhang, K. Luo, Y. Gao, F. Ling, X. Chen, Z. Zhao, and D. Yu, *Physics Letters A*, 126525 (2020).
- [123] H. Yamada, C. Liu, S. Wu, Y. Koyama, S. Ju, J. Shiomi, J. Morikawa, and R. Yoshida, *ACS central science* **5**, 1717 (2019).
- [124] G. Kresse and J. Hafner, *Physical Review B* **47**, 558 (1993).
- [125] G. Kresse and J. Hafner, *Physical Review B* **49**, 14251 (1994).
- [126] G. Kresse and J. Furthmüller, *Computational materials science* **6**, 15 (1996).
- [127] G. Kresse and J. Furthmüller, *Physical review B* **54**, 11169 (1996).
- [128] T. Chen, T. He, M. Benesty, V. Khotilovich, Y. Tang, H. Cho, *et al.*, *R package version 0.4-2* **1** (2015).
- [129] C. W. Glass, A. R. Oganov, and N. Hansen, *Computer physics communications* **175**, 713 (2006).
- [130] J. A. Flores-Livas, L. Boeri, A. Sanna, G. Profeta, R. Arita, and M. Eremets, *Physics Reports* **856**, 1 (2020), a perspective on conventional high-temperature superconductors at high pressure: Methods and materials.
- [131] D. V. Semenok, A. G. Kvashnin, A. G. Ivanova, V. Svitlyk, V. Y. Fominski, A. V. Sadakov, O. A. Sobolevskiy, V. M. Pudalov, I. A. Troyan, and A. R. Oganov, *Materials Today* **33**, 36 (2020).
- [132] L. Boeri and G. B. Bachelet, *Journal of Physics: Condensed Matter* **31**, 234002 (2019).
- [133] J. A. Flores-Livas and R. Arita, *Physics* **12**, 96 (2019).
- [134] H. Wang, X. Li, G. Gao, Y. Li, and Y. Ma, *Wiley Interdisciplinary Reviews: Computational Molecular Science* **8**, e1330 (2018).
- [135] B. Li, Z. Miao, L. Ti, S. Liu, J. Chen, Z. Shi, and E. Gregoryanz, *Journal of Applied Physics* **126**, 235901 (2019).
- [136] N. Bernstein, C. S. Hellberg, M. Johannes, I. Mazin, and M. Mehl, *Physical Review B* **91**, 060511 (2015).
- [137] I. A. Kruglov, A. G. Kvashnin, A. F. Goncharov, A. R. Oganov, S. S. Lobanov, N. Holtgrewe, S. Jiang, V. B. Prakapenka, E. Greenberg, and A. V. Yanilkin, *Science advances* **4**, eaat9776 (2018).
- [138] A. Matasov and V. Krasavina, *SN Applied Sciences* **2**, 1 (2020).
- [139] F. Pedregosa, G. Varoquaux, A. Gramfort, V. Michel, B. Thirion, O. Grisel, M. Blondel, P. Prettenhofer, R. Weiss, V. Dubourg, *et al.*, *the Journal of machine Learning research* **12**, 2825 (2011).
- [140] T. Hastie, R. Tibshirani, and J. Friedman, *The Elements of Statistical Learning*, Springer Series in Statistics (Springer New York Inc., New York, NY, USA, 2001).
- [141] C. M. Bishop, *Pattern Recognition and Machine Learning* (Springer, 2006).
- [142] R. Tibshirani, *Journal of the Royal Statistical Society. Series B (Methodological)* **58**, 267 (1996).
- [143] T. Yoshida, K. Hongo, and R. Maezono, *The Journal of Physical Chemistry C* **123**, 14126 (2019).
- [144] T. Yoshida, R. Maezono, and K. Hongo, *ACS omega* **5**, 13403 (2020).
- [145] H. Zou and T. Hastie, *Journal of the Royal Statistical Society. Series B (Statistical Methodology)* **67**, 301 (2005).
- [146] P. B. de Castro, K. Terashima, T. D. Yamamoto, Z. Hou, S. Iwasaki, R. Matsumoto, S. Adachi, Y. Saito, P. Song, H. Takeya, *et al.*, *NPG Asia Materials* **12**, 1 (2020).
- [147] T. Yoshida, R. Maezono, and K. Hongo, *ACS Applied Nano Materials* **4**, 1932 (2021), <https://doi.org/10.1021/acsnm.0c03298>.
- [148] J. Bergstra, B. Komer, C. Eliasmith, D. Yamins, and D. D. Cox, *Computational Science & Discovery* **8**, 014008 (2015).
- [149] J. P. Perdew, K. Burke, and M. Ernzerhof, *Physical review letters* **77**, 3865 (1996).
- [150] A. Togo and I. Tanaka, *Scr. Mater.* **108**, 1 (2015).
- [151] K. Nakano, K. Hongo, and R. Maezono, *Inorganic chemistry* **56**, 13732 (2017).
- [152] K. Nakano, K. Hongo, and R. Maezono, *Scientific reports* **6**, 1 (2016).
- [153] N. Marzari, D. Vanderbilt, A. De Vita, and M. Payne, *Physical review letters* **82**, 3296 (1999).
- [154] S. Baroni, S. De Gironcoli, A. Dal Corso, and P. Giannozzi, *Reviews of modern Physics* **73**, 515 (2001).
- [155] P. Giannozzi, S. Baroni, N. Bonini, M. Calandra, R. Car, C. Cavazzoni, D. Ceresoli, G. L. Chiarotti, M. Cococcioni, I. Dabo, *et al.*, *J. Phys. Condens. Matter.* **21**, 395502 (2009).



## SUPPLEMENTAL INFORMATION

### *Ab initio* calculations

The crystal structures predicted for  $\text{YKH}_{12}$  and  $\text{LaKH}_{12}$  at each pressure are given in Table. III. For electronic structure calculations (required to get pressure-dependent DOS) and phonon calculations (to evaluate dynamical stabilities), we used VASP package [124–127] with GGA-PBE exchange-correlation functionals. [149] Ionic cores are described by ultrasoft pseudo potentials provided in the package. To assist the convergence in the self-consistent field iterations, we used Marzari-Vanderbilt smearing scheme. [153] Resolutions for the plane wave basis set expansions [Energy cutoff ( $E_{\text{cut}}$ )] and the Brillouin-zone integration [ $k$ -mesh] were determined so that the resultant energy values could converge within the required accuracies, finally getting  $E_{\text{cut}}=75$  Ry with  $(8 \times 8 \times 8)$   $k$ -mesh for the electronic Brillouin-zone. Phonon calculations are performed by linear-response method [154] with  $(4 \times 4 \times 4)$   $q$ -mesh.

To estimate  $T_c$ , we used Allen-Dynes formula implemented in Quantum Espresso package [155] with the effective Coulomb interaction  $\mu^*$  being chosen 0.1 empirically. Denser  $k$ -meshes,  $16 \times 16 \times 16$ , were used for the double-delta integrations in electron-phonon calculations. The estimated results are summarized in Table IV.

### Descriptors

Total 84 descriptors used for the regression are listed in Table V, corresponding to those for (i) [space group], (ii) [pressure], and (iii) [chemical composition]. A descriptor for a composition is composed from that for each atomic species in various way. Denoting  $\alpha$  as the index specifying atomic species, and  $f_\alpha$  as the descriptor for  $\alpha$ ,

$$\begin{aligned}
 f_{\text{ave}} &= \sum_{\alpha} W_{\alpha}^* \cdot f_{\alpha} , \\
 f_{\text{sum}} &= \sum_{\alpha} W_{\alpha} \cdot f_{\alpha} , \\
 f_{\text{var}} &= \sum_{\alpha} W_{\alpha}^* \cdot (f_{\alpha} - f_{\text{ave}})^2 , \\
 f_{\text{max}} &= \max_{\alpha} \{f_{\alpha}\} , \\
 f_{\text{min}} &= \min_{\alpha} \{f_{\alpha}\} ,
 \end{aligned} \tag{1}$$

are used, where  $W_{\alpha}$  is the number of  $\alpha$ -species included in the composition, and  $W_{\alpha}^*$  is the normalized fraction.

### List of estimated and training data

Total 426 training data used to construct the regression are listed in Table VII. By using the XGBoost regression, we es-

timated  $T_c$  for a set of chemical compositions as shown in Table VI.

TABLE III. Crystal structures of  $\text{YKH}_{12}$  and  $\text{LaKH}_{12}$  predicted at each pressure ( $P$ ). Lattice parameters ( $a$ ,  $b$  and  $c$ ) are given in unit of  $\text{\AA}$ .

		$P$ (GPa)		Atomic coordinates (fractional)			
				Atoms	$x$	$y$	$z$
$\text{YKH}_{12}$	$C2/m$	240	$a = 4.685$	K(2c)	0.00000	0.00000	0.50000
			$b = 4.959$	Y(2b)	0.00000	0.50000	0.00000
			$c = 3.412$	H(8j)	0.10546	0.13491	0.02245
			$\alpha = \gamma = 90^\circ$	H(8j)	0.11840	0.35886	0.52932
			$\beta = 94.640^\circ$	H(8j)	0.24652	0.27559	0.74033
$\text{LaKH}_{12}$	$R\bar{3}m$	140	$a = b = 5.457$	K(3b)	0.00000	0.00000	0.50000
			$c = 5.844$	La(3a)	0.00000	0.00000	0.00000
			$\alpha = \beta = 90^\circ$	H(36i)	0.00522	0.29080	0.25260
			$\gamma = 120^\circ$				
$\text{LaKH}_{12}$	$C2/m$	250		K(4i)	0.12534	0.00000	0.82783
				La(4i)	0.12649	0.50000	0.34168
			$a = 8.126$	H(8j)	0.11445	0.17656	0.45546
			$b = 5.479$	H(8j)	0.11651	0.10279	0.25125
			$c = 4.379$	H(8j)	0.12613	0.30763	0.96974
			$\alpha = \gamma = 90^\circ$	H(8j)	0.13714	0.36984	0.78838
			$\beta = 122.253^\circ$	H(8j)	0.24797	0.21751	0.24331
				H(4g)	0.00000	0.21727	0.00000
	H(4h)	0.00000	0.26959	0.50000			

TABLE IV.  $T_c$  estimated by Allen-Dynes formula using *ab initio* phonon calculations for  $\text{YKH}_{12}$  [ $C2/m$ ] and  $\text{LaKH}_{12}$  [ $R\bar{3}m$ ] at each pressure.  $\lambda$  and  $\omega_{\log}$  are the parameters appearing in the formula.

	$P$ [GPa]	$\lambda$	$\omega_{\log}$ [K]	$T_c$ [K]
$\text{YKH}_{12}$	180	1.398	1289.465	137.1
$\text{YKH}_{12}$	200	1.400	1324.987	141.1
$\text{YKH}_{12}$	240	1.427	1318.072	143.2
$\text{YKH}_{12}$	260	1.436	1127.344	123.2
$\text{YKH}_{12}$	300	1.587	911.696	109.4
$\text{LaKH}_{12}$	140	1.531	854.12	99.2
$\text{LaKH}_{12}$	160	1.665	789.38	98.8

TABLE V. Total 84 descriptors used for the regression, corresponding to those for (i) [space group], (ii) [pressure], and (iii) [chemical composition]. Each weighting scheme (ave/sum/var/max/min) is defined in Eqs.(1).

Weighting scheme	Property	Label	Description
ave	(i)	atomic_radius_rahm	Atomic radius by Rahm <i>et al.</i>
ave	(i)	boiling_point	Boiling temperature
ave	(i)	covalent_radius_cordero	Covalent radius by Cordero <i>et al.</i>
ave	(i)	covalent_radius_pyykko	Single bond covalent radius by Pyykko <i>et al.</i>
ave/max	(i)	covalent_radius_slater	Covalent radius by Slater
ave	(i)	en_allen	Allen's scale of electronegativity
ave/sum	(i)	en_ghosh	Ghosh's scale of electronegativity
ave/sum	(i)	first_ion_en	First ionisation energy
ave	(i)	fusion_enthalpy	Fusion heat
ave/sum/var	(i)	gs_bandgap	DFT bandgap energy of $T = 0$ K ground state
ave/max	(i)	gs_volume_per	DFT volume per atom of $T = 0$ K ground state
ave/sum/var/max/min	(i)	hhi_p	Herfindahl-Hirschman Index (HHI) production values
ave/max/min	(i)	hhi_r	Herfindahl-Hirschman Index (HHI) reserves values
ave/sum/var	(i)	heat_capacity_mass	Mass specific heat capacity
ave	(i)	evaporation_heat	Evaporation heat
ave/var/max/min	(i)	lattice_constant	Physical dimension of unit cells in a crystal lattice
ave/min	(i)	mendeleviev_number	Atom number in mendeleviev's periodic table
ave/sum	(i)	melting_point	Melting point
ave/sum/max	(i)	molar_volume	Molar volume
ave/sum/max	(i)	num_unfilled	Total unfilled electron
ave/var/max	(i)	num_valance	Total valance electron
ave	(i)	period	Period in the periodic table
ave	(i)	vdw_radius	Van der Waals radius
ave/max	(i)	vdw_radius_alvarez	Van der Waals radius according to Alvarez
ave/max	(i)	vdw_radius_mm3	Van der Waals radius from the MM3 FF
sum	(i)	atomic_radius	Atomic radius
sum	(i)	atomic_volume	Atomic volume
sum	(i)	c6_gb	C <sub>6</sub> dispersion coefficient in a.u
sum/max	(i)	covalent_radius_pyykko_triple	Triple bond covalent radius by Pyykko <i>et al.</i>
sum/min	(i)	electron_negativity	Tendency of an atom to attract a shared pair of electrons
var/min	(i)	en_pauling	Mulliken's scale of electronegativity
sum/max	(i)	gs_est_bcc_latent	Estimated BCC lattice parameter based on the DFT volume
sum/var	(i)	num_s_unfilled	Unfilled electron in s shell
sum	(i)	specific_heat	Specific heat at 20oC
var	(i)	icsd_volume	Atom volume in ICSD database
var/max	(i)	vdw_radius_uff	Van der Waals radius from the UFF
max/min	(i)	bulk_modulus	Bulk modulus
max	(i)	num_p_unfilled	Unfilled electron in p shell
ave/var/min	(ii)	s_dos	Density of states of s electron at Fermi surface (state/eV/atom)
ave/min	(ii)	Free_energy	Pressure-related free energy
var/max/sum	(ii)	p_dos	Density of states of p electron at Fermi surface (state/eV/atom)
max/sum	(ii)	element_dos	Density of states at Fermi surface (state/eV/atom)
	(iii)	spg_number	space group number

TABLE VI. 28 chemical compositions to estimate  $T_c$  by using the XGBoost regression learned with the 426 training data.

No.		$T_c$ [K]	No.		$T_c$ [K]
1	YKH <sub>12</sub>	168.93	15	LaSH <sub>12</sub>	74.94
2	LaKH <sub>12</sub>	162.85	16	LaArH <sub>12</sub>	74.91
3	YClH <sub>12</sub>	137.60	17	YBiH <sub>12</sub>	72.54
4	LaMgH <sub>12</sub>	135.33	18	YFeH <sub>12</sub>	64.58
5	LaClH <sub>12</sub>	132.70	19	LaPH <sub>12</sub>	60.59
6	LaAcH <sub>12</sub>	128.99	20	YTaH <sub>12</sub>	58.93
7	YSeH <sub>12</sub>	127.01	21	YTiH <sub>12</sub>	57.21
8	YSH <sub>12</sub>	123.04	22	LaBiH <sub>12</sub>	56.59
9	YArH <sub>12</sub>	99.59	23	LaSbH <sub>12</sub>	52.38
10	YGeH <sub>12</sub>	98.60	24	LaSiH <sub>12</sub>	50.53
11	LaSe <sub>12</sub>	98.25	25	LaTaH <sub>12</sub>	42.25
12	YInH <sub>12</sub>	93.81	26	LaTiH <sub>12</sub>	39.85
13	YPH <sub>12</sub>	92.78	27	LaFeH <sub>12</sub>	24.48
14	LaTeH <sub>12</sub>	77.93	28	LaGeH <sub>12</sub>	18.47

TABLE VII: Total 533 training data [7, 9, 11–15, 18–26, 35–122] used to construct our regressors (see the main text). The label 'Spg' abbreviates 'Space group' with the numbering.  $\mu$  is the parameter for the effective Coulomb interactions appearing in Allen-Dynes formula.

No.		Spg.	$P$ (GPa)	$T_c$ (K)	$\mu$
0	SiH <sub>4</sub>	64 <i>Cmca</i>	60.0	75.0	0.1
1	SiH <sub>4</sub>	64 <i>Cmca</i>	150.0	20.0	0.1
2	SiH <sub>4</sub>	64 <i>Cmca</i>	200.0	30.0	0.1
3	SiH <sub>4</sub>	64 <i>Cmca</i>	250.0	50.0	0.1
4	YH <sub>3</sub>	225 <i>Fm<math>\bar{3}</math>m</i>	17.7	40.0	0.1
5	YH <sub>3</sub>	225 <i>Fm<math>\bar{3}</math>m</i>	28.0	9.0	0.1
6	YH <sub>3</sub>	225 <i>Fm<math>\bar{3}</math>m</i>	35.0	0.0	0.1
7	YH <sub>3</sub>	225 <i>Fm<math>\bar{3}</math>m</i>	45.0	0.0	0.1
8	YH <sub>3</sub>	225 <i>Fm<math>\bar{3}</math>m</i>	52.0	6.0	0.1
9	YH <sub>3</sub>	225 <i>Fm<math>\bar{3}</math>m</i>	62.0	5.0	0.1
10	YH <sub>3</sub>	225 <i>Fm<math>\bar{3}</math>m</i>	67.0	4.0	0.1
11	YH <sub>3</sub>	225 <i>Fm<math>\bar{3}</math>m</i>	74.0	3.0	0.1
12	BaH <sub>2</sub>	194 <i>P6<sub>3</sub>/mmc</i>	60.0	4.0	0.1
13	Si <sub>2</sub> H <sub>6</sub>	2 <i>P<math>\bar{1}</math></i>	175.0	65.0	0.1
14	Si <sub>2</sub> H <sub>6</sub>	2 <i>P<math>\bar{1}</math></i>	200.0	80.0	0.1
15	Si <sub>2</sub> H <sub>6</sub>	221 <i>Pm<math>\bar{3}</math>m</i>	275.0	139.0	0.1
16	Si <sub>2</sub> H <sub>6</sub>	15 <i>C2/c</i>	300.0	34.0	0.1
17	SiH <sub>8</sub>	68 <i>Ccca</i>	250.0	107.0	0.1
18	SiH <sub>4</sub>	40 <i>Ama2</i>	120.0	22.0	0.1
19	SiH <sub>4</sub>	194 <i>P6<sub>3</sub>/mmc</i>	200.0	62.0	0.1
20	HBr	11 <i>P2<sub>1</sub>/m</i>	140.0	28.0	0.1
21	HBr	11 <i>P2<sub>1</sub>/m</i>	160.0	34.0	0.1
22	HBr	11 <i>P2<sub>1</sub>/m</i>	180.0	49.0	0.1
23	HBr	11 <i>P2<sub>1</sub>/m</i>	200.0	51.0	0.1
24	HCl	11 <i>P2<sub>1</sub>/m</i>	240.0	7.0	0.1
25	HCl	11 <i>P2<sub>1</sub>/m</i>	280.0	14.0	0.1
26	HCl	11 <i>P2<sub>1</sub>/m</i>	320.0	30.0	0.1
27	HCl	11 <i>P2<sub>1</sub>/m</i>	360.0	41.0	0.1
28	GaH <sub>3</sub>	223 <i>Pm<math>\bar{3}</math>n</i>	120.0	102.0	0.1
29	GaH <sub>3</sub>	223 <i>Pm<math>\bar{3}</math>n</i>	160.0	86.0	0.1
30	GaH <sub>3</sub>	223 <i>Pm<math>\bar{3}</math>n</i>	200.0	72.0	0.1
31	GaH <sub>3</sub>	223 <i>Pm<math>\bar{3}</math>n</i>	240.0	60.0	0.1
32	PtH <sub>3</sub>	225 <i>Fm<math>\bar{3}</math>m</i>	77.0	25.0	0.1
33	PtH	225 <i>Fm<math>\bar{3}</math>m</i>	90.0	13.0	0.1
34	PtH	225 <i>Fm<math>\bar{3}</math>m</i>	115.0	5.0	0.1
35	PtH	225 <i>Fm<math>\bar{3}</math>m</i>	145.0	4.0	0.1
36	B <sub>2</sub> H <sub>6</sub>	63 <i>Cmcm</i>	360.0	125.0	0.13
37	GeH <sub>8</sub>	14 <i>P2<sub>1</sub>/c</i>	250.0	90.0	0.1
38	PtH	225 <i>Fm<math>\bar{3}</math>m</i>	88.0	24.0	0.1
39	PtH	225 <i>Fm<math>\bar{3}</math>m</i>	95.0	18.0	0.1
40	PtH	194 <i>P6<sub>3</sub>/mmc</i>	105.0	16.0	0.1
41	PtH	194 <i>P6<sub>3</sub>/mmc</i>	120.0	10.0	0.1
42	PtH	225 <i>Fm<math>\bar{3}</math>m</i>	140.0	6.0	0.1
43	PtH	225 <i>Fm<math>\bar{3}</math>m</i>	160.0	5.0	0.1
44	PtH	225 <i>Fm<math>\bar{3}</math>m</i>	200.0	3.0	0.1
45	KH <sub>6</sub>	15 <i>C2/c</i>	166.0	70.0	0.1
46	KH <sub>6</sub>	15 <i>C2/c</i>	230.0	70.0	0.1
47	KH <sub>6</sub>	15 <i>C2/c</i>	300.0	46.0	0.1
48	NbH	66 <i>Cccm</i>	0.0001	2.4	0.1
49	NbH <sub>2</sub>	225 <i>Fm<math>\bar{3}</math>m</i>	0.0001	2.6	0.1
50	NbH <sub>2</sub>	225 <i>Fm<math>\bar{3}</math>m</i>	50.0	1.5	0.1
51	NbH <sub>4</sub>	139 <i>I4/mmm</i>	300.0	47.0	0.1
52	GeH <sub>3</sub>	223 <i>Pm<math>\bar{3}</math>n</i>	180.0	160.0	0.1
53	GeH <sub>3</sub>	131 <i>P42/mmc</i>	180.0	110.0	0.1
54	GeH <sub>3</sub>	66 <i>Cccm</i>	180.0	100.0	0.1
55	BaH <sub>6</sub>	123 <i>P4/mmm</i>	100.0	38.0	0.1
56	MgH <sub>2</sub>	194 <i>P6<sub>3</sub>/mmc</i>	180.0	24.0	0.1
57	MgH <sub>4</sub>	63 <i>Cmcm</i>	100.0	38.0	0.1

58	MgH <sub>12</sub>	146 <i>R3</i>	140.0	60.0	0.1
59	BH	191 <i>P6/mmm</i>	100.0	39.0	0.1
60	BH	191 <i>P6/mmm</i>	125.0	32.0	0.1
61	BH	191 <i>P6/mmm</i>	150.0	27.0	0.1
62	BH	191 <i>P6/mmm</i>	175.0	21.0	0.1
63	BH	191 <i>P6/mmm</i>	200.0	19.0	0.1
64	LiH <sub>2</sub>	127 <i>P4/mbm</i>	150.0	0.0	0.13
65	LiH <sub>6</sub>	166 <i>R3m</i>	150.0	38.34	0.13
66	LiH <sub>6</sub>	166 <i>R3m</i>	200.0	42.0	0.13
67	LiH <sub>6</sub>	166 <i>R3m</i>	250.0	58.0	0.13
68	LiH <sub>6</sub>	166 <i>R3m</i>	300.0	82.0	0.13
69	LiH <sub>8</sub>	97 <i>I422</i>	100.0	31.04	0.13
70	LiH <sub>8</sub>	97 <i>I422</i>	150.0	35.0	0.13
71	LiH <sub>8</sub>	97 <i>I422</i>	200.0	37.0	0.13
72	BeH <sub>2</sub>	63 <i>Cmcm</i>	250.0	44.0	0.1
73	BeH <sub>2</sub>	63 <i>Cmcm</i>	230.0	42.0	0.1
74	BeH <sub>2</sub>	63 <i>Cmcm</i>	270.0	45.0	0.1
75	BeH <sub>2</sub>	63 <i>Cmcm</i>	290.0	37.0	0.1
76	BeH <sub>2</sub>	63 <i>Cmcm</i>	310.0	33.0	0.1
77	BeH <sub>2</sub>	129 <i>P4/nmm</i>	350.0	39.0	0.1
78	BeH <sub>2</sub>	129 <i>P4/nmm</i>	365.0	50.0	0.1
79	BeH <sub>2</sub>	129 <i>P4/nmm</i>	390.0	30.0	0.1
80	H <sub>2</sub> S	2 <i>P1</i>	130.0	33.0	0.13
81	H <sub>2</sub> S	2 <i>P1</i>	140.0	40.0	0.13
82	H <sub>2</sub> S	2 <i>P1</i>	150.0	56.0	0.13
83	H <sub>2</sub> S	2 <i>P1</i>	158.0	60.0	0.13
84	H <sub>2</sub> S	64 <i>Cmca</i>	160.0	82.0	0.13
85	H <sub>2</sub> S	64 <i>Cmca</i>	170.0	75.0	0.13
86	H <sub>2</sub> S	64 <i>Cmca</i>	180.0	65.0	0.13
87	BeH <sub>2</sub>	63 <i>Cmcm</i>	300.0	45.0	0.1
88	VH <sub>2</sub>	225 <i>Fm3m</i>	0.0	0.5	0.1
89	VH <sub>2</sub>	62 <i>Pnma</i>	60.0	4.0	0.1
90	NbH <sub>2</sub>	225 <i>Fm3m</i>	0.0	1.5	0.1
91	NbH <sub>2</sub>	186 <i>P6<sub>3</sub>mc</i>	60.0	0.5	0.1
92	H <sub>3</sub> S	160 <i>R3m</i>	130.0	166.0	0.1
93	H <sub>3</sub> S	229 <i>Im3m</i>	200.0	191.0	0.1
94	H <sub>3</sub> S	229 <i>Im3m</i>	250.0	179.0	0.1
95	XeH	71 <i>Immm</i>	100.0	29.0	0.12
96	XeH	71 <i>Immm</i>	200.0	17.0	0.12
97	XeH	71 <i>Immm</i>	300.0	13.0	0.12
98	XeH <sub>2</sub>	63 <i>Cmcm</i>	400.0	26.0	0.12
99	XeH <sub>2</sub>	63 <i>Cmcm</i>	500.0	20.0	0.12
100	XeH <sub>2</sub>	63 <i>Cmcm</i>	600.0	16.0	0.12
101	AlH <sub>5</sub>	11 <i>P2<sub>1</sub>/m-Z</i>	250.0	146.0	0.1
102	H <sub>2</sub> I	62 <i>Pnma</i>	100.0	5.3	0.1
103	H <sub>2</sub> I	62 <i>Pnma</i>	150.0	4.32	0.1
104	H <sub>2</sub> I	62 <i>Pnma</i>	200.0	3.67	0.1
105	H <sub>2</sub> I	62 <i>Pnma</i>	240.0	3.77	0.1
106	H <sub>2</sub> I	166 <i>R3m</i>	240.0	33.05	0.1
107	H <sub>2</sub> I	166 <i>R3m</i>	260.0	30.82	0.1
108	H <sub>2</sub> I	166 <i>R3m</i>	300.0	25.09	0.1
109	H <sub>4</sub> I	191 <i>P6/mmm</i>	120.0	9.92	0.1
110	H <sub>4</sub> I	191 <i>P6/mmm</i>	160.0	8.8	0.1
111	H <sub>4</sub> I	191 <i>P6/mmm</i>	200.0	9.57	0.1
112	H <sub>4</sub> I	191 <i>P6/mmm</i>	250.0	11.26	0.1
113	H <sub>4</sub> I	191 <i>P6/mmm</i>	300.0	12.48	0.1
114	GeH <sub>4</sub>	40 <i>Ama2</i>	250.0	57.0	0.1
115	GeH <sub>4</sub>	15 <i>C2/c</i>	500.0	84.0	0.1
116	OsH	225 <i>Fm3m</i>	100.0	2.1	0.1
117	H <sub>2</sub> I	63 <i>Cmcm</i>	100.0	7.8	0.1
118	H <sub>4</sub> I	191 <i>P6/mmm</i>	100.0	17.5	0.1
119	H <sub>4</sub> I	191 <i>P6/mmm</i>	150.0	20.4	0.1
120	InH <sub>3</sub>	148 <i>R3</i>	200.0	40.5	0.1

121	InH <sub>3</sub>	148 $R\bar{3}$	250.0	39.0	0.1
122	InH <sub>3</sub>	148 $R\bar{3}$	300.0	38.0	0.1
123	InH <sub>5</sub>	11 $P2_1/m$	150.0	27.0	0.1
124	InH <sub>5</sub>	11 $P2_1/m$	200.0	40.5	0.1
125	HCl	12 $C2/m$	250.0	20.0	0.1
126	HBr	12 $C2/m$	120.0	0.01	0.1
127	BiH	194 $P6_3/mmc$	250.0	30.0	0.1
128	BiH	194 $P6_3/mmc$	300.0	20.0	0.1
129	BiH <sub>2</sub>	11 $P2_1/m$	150.0	59.0	0.1
130	BiH <sub>2</sub>	11 $P2_1/m$	200.0	60.0	0.1
131	BiH <sub>2</sub>	11 $P2_1/m$	250.0	63.0	0.1
132	BiH <sub>2</sub>	11 $P2_1/m$	300.0	65.0	0.1
133	BiH <sub>4</sub>	59 $Pmnn$	150.0	93.0	0.1
134	BiH <sub>4</sub>	59 $Pmnn$	200.0	88.0	0.1
135	BiH <sub>4</sub>	59 $Pmnn$	250.0	77.0	0.1
136	BiH <sub>4</sub>	59 $Pmnn$	300.0	75.0	0.1
137	BiH <sub>5</sub>	12 $C2/m$	200.0	103.0	0.1
138	BiH <sub>5</sub>	12 $C2/m$	250.0	101.0	0.1
139	BiH <sub>5</sub>	12 $C2/m$	300.0	119.0	0.1
140	BiH <sub>6</sub>	2 $P\bar{1}$	200.0	100.0	0.1
141	BiH <sub>6</sub>	2 $P\bar{1}$	250.0	107.0	0.1
142	BiH <sub>6</sub>	2 $P\bar{1}$	300.0	113.0	0.1
143	MgH <sub>6</sub>	229 $Im\bar{3}m$	300.0	263.0	0.12
144	MgH <sub>6</sub>	229 $Im\bar{3}m$	350.0	260.0	0.12
145	MgH <sub>6</sub>	229 $Im\bar{3}m$	400.0	271.0	0.12
146	HSe <sub>2</sub>	12 $C2/m$	300.0	5.0	0.1
147	HSe	14 $P2_1/c$	300.0	23.0	0.1
148	HSe	129 $P4/nmm$	250.0	39.0	0.1
149	HSe	129 $P4/nmm$	300.0	42.0	0.1
150	H <sub>3</sub> Se	229 $Im\bar{3}m$	200.0	116.0	0.1
151	H <sub>3</sub> Se	229 $Im\bar{3}m$	250.0	111.0	0.1
152	H <sub>3</sub> Se	229 $Im\bar{3}m$	300.0	110.0	0.1
153	H <sub>3</sub> S	229 $Im\bar{3}m$	300.0	160.0	0.1
154	HfH <sub>2</sub>	139 $I4/mmm$	0.0001	0.192	0.1
155	HfH <sub>2</sub>	139 $I4/mmm$	10.0	0.081	0.1
156	HfH <sub>2</sub>	139 $I4/mmm$	30.0	0.021	0.1
157	HfH <sub>2</sub>	139 $I4/mmm$	50.0	0.008	0.1
158	HfH <sub>2</sub>	67 $Cmma$	180.0	8.159	0.1
159	HfH <sub>2</sub>	67 $Cmma$	240.0	6.207	0.1
160	HfH <sub>2</sub>	11 $P2_1/m$	260.0	12.804	0.1
161	HfH <sub>2</sub>	11 $P2_1/m$	280.0	7.962	0.1
162	CrH	194 $P6_3/mmc$	0.0	10.6	0.1
163	CrH	194 $P6_3/mmc$	60.0	4.3	0.1
164	CrH	194 $P6_3/mmc$	120.0	3.3	0.1
165	CrH	194 $P6_3/mmc$	200.0	3.1	0.1
166	CrH <sub>3</sub>	194 $P6_3/mmc$	81.0	37.1	0.1
167	CrH <sub>3</sub>	194 $P6_3/mmc$	120.0	29.5	0.1
168	CrH <sub>3</sub>	194 $P6_3/mmc$	160.0	28.2	0.1
169	CrH <sub>3</sub>	194 $P6_3/mmc$	200.0	27.2	0.1
170	PbH <sub>8</sub>	12 $C2/m$	138.0	76.0	0.1
171	PbH <sub>8</sub>	12 $C2/m$	180.0	97.0	0.1
172	PbH <sub>8</sub>	12 $C2/m$	230.0	107.0	0.1
173	PbH <sub>8</sub>	12 $C2/m$	250.0	106.0	0.1
174	PbH <sub>8</sub>	12 $C2/m$	300.0	104.0	0.1
175	PbH <sub>8</sub>	12 $C2/m$	350.0	103.0	0.1
176	SiH <sub>4</sub>	15 $C2/c$	300.0	29.65	0.13
177	SiH <sub>4</sub>	14 $P2_1/c$	400.0	31.57	0.13
178	SiH <sub>4</sub>	12 $C2/m$	610.0	106.31	0.13
179	HS <sub>2</sub>	15 $C2/c$	200.0	35.3	0.1
180	HS <sub>2</sub>	12 $C2/m$	250.0	25.1	0.1
181	HS	12 $C2/m$	300.0	38.0	0.1
182	H <sub>5</sub> S <sub>2</sub>	1 $P1$	112.0	70.1	0.1
183	H <sub>5</sub> S <sub>2</sub>	1 $P1$	120.0	75.2	0.1
184	H <sub>5</sub> S <sub>2</sub>	1 $P1$	130.0	79.1	0.1



185	SnH <sub>4</sub>	139 <i>I4/mmm</i>	220.0	91.0	0.1
186	SnH <sub>8</sub>	119 <i>I4/m2</i>	220.0	81.0	0.1
187	SnH <sub>12</sub>	12 <i>C2/m</i>	250.0	93.0	0.1
188	SnH <sub>14</sub>	12 <i>C2/m</i>	300.0	97.0	0.1
189	Fe <sub>2</sub> SH <sub>3</sub>	36 <i>Cmc21</i>	173.0	0.3	0.1
190	AsH	63 <i>Cmcm</i>	300.0	21.2	0.1
191	AsH	63 <i>Cmcm</i>	400.0	20.2	0.1
192	AsH <sub>8</sub>	15 <i>C2/c</i>	350.0	141.0	0.1
193	AsH <sub>8</sub>	15 <i>C2/c</i>	400.0	143.9	0.1
194	AsH <sub>8</sub>	15 <i>C2/c</i>	450.0	151.4	0.1
195	SbH	62 <i>Pnma</i>	175.0	14.6	0.1
196	SbH	62 <i>Pnma</i>	215.0	10.5	0.1
197	SbH	62 <i>Pnma</i>	255.0	8.5	0.1
198	SbH	62 <i>Pnma</i>	295.0	6.8	0.1
199	SbH <sub>3</sub>	47 <i>Pmmm</i>	300.0	25.9	0.1
200	SbH <sub>3</sub>	47 <i>Pmmm</i>	400.0	19.8	0.1
201	SbH <sub>4</sub>	194 <i>P6<sub>3</sub>/mmc</i>	150.0	102.2	0.1
202	SbH <sub>4</sub>	194 <i>P6<sub>3</sub>/mmc</i>	200.0	102.3	0.1
203	SbH <sub>4</sub>	194 <i>P6<sub>3</sub>/mmc</i>	250.0	99.9	0.1
204	SbH <sub>4</sub>	194 <i>P6<sub>3</sub>/mmc</i>	300.0	93.9	0.1
205	PH <sub>2</sub>	12 <i>C2/m</i>	100.0	49.01	0.1
206	PH <sub>2</sub>	12 <i>C2/m</i>	150.0	55.52	0.1
207	PH <sub>2</sub>	12 <i>C2/m</i>	200.0	75.59	0.1
208	PH <sub>2</sub>	139 <i>I4/mmm</i>	100.0	32.47	0.1
209	PH <sub>2</sub>	139 <i>I4/mmm</i>	150.0	50.6	0.1
210	PH <sub>2</sub>	139 <i>I4/mmm</i>	200.0	70.36	0.1
211	RuH	225 <i>Fm<math>\bar{3}</math>m</i>	100.0	0.41	0.1
212	RuH <sub>3</sub>	221 <i>Pm<math>\bar{3}</math>m</i>	100.0	3.57	0.1
213	RuH <sub>3</sub>	223 <i>Pm<math>\bar{3}</math>n</i>	200.0	1.25	0.1
214	TcH <sub>2</sub>	139 <i>I4/mmm</i>	100.0	5.42	0.1
215	TcH <sub>2</sub>	139 <i>I4/mmm</i>	150.0	6.31	0.1
216	TcH <sub>2</sub>	139 <i>I4/mmm</i>	200.0	10.65	0.1
217	TcH <sub>2</sub>	63 <i>Cmcm</i>	300.0	8.61	0.1
218	TcH <sub>3</sub>	131 <i>P4<sub>2</sub>/mmc</i>	300.0	9.94	0.1
219	H <sub>4</sub> Te	191 <i>P6/mmm</i>	170.0	104.47	0.1
220	H <sub>4</sub> Te	191 <i>P6/mmm</i>	200.0	99.18	0.1
221	H <sub>4</sub> Te	191 <i>P6/mmm</i>	230.0	91.33	0.1
222	H <sub>4</sub> Te	166 <i>R<math>\bar{3}</math>m</i>	270.0	75.66	0.1
223	H <sub>4</sub> Te	166 <i>R<math>\bar{3}</math>m</i>	300.0	67.7	0.1
224	H <sub>5</sub> Te <sub>2</sub>	12 <i>C2/m</i>	200.0	57.98	0.1
225	H <sub>5</sub> Te <sub>2</sub>	12 <i>C2/m</i>	300.0	46.0	0.1
226	HTe	129 <i>P4/nmm</i>	150.0	28.28	0.1
227	HTe	129 <i>P4/nmm</i>	200.0	18.71	0.1
228	HTe	194 <i>P6<sub>3</sub>/mmc</i>	300.0	44.26	0.1
229	H <sub>4</sub> S <sub>3</sub>	62 <i>Pnma</i>	140.0	2.1	0.13
230	KAuH <sub>2</sub>	123 <i>P4/mmm</i>	120.0	0.28	0.11
231	Ba(AuH <sub>2</sub> ) <sub>2</sub>	79 <i>I4</i>	0.0001	30.0	0.11
232	Sr(AuH <sub>2</sub> ) <sub>2</sub>	79 <i>I4</i>	0.0001	10.0	0.11
233	MgGeH <sub>6</sub>	200 <i>Pm<math>\bar{3}</math></i>	200.0	66.6	0.1
234	MgGeH <sub>6</sub>	200 <i>Pm<math>\bar{3}</math></i>	250.0	59.05	0.1
235	MgGeH <sub>6</sub>	200 <i>Pm<math>\bar{3}</math></i>	300.0	50.29	0.1
236	MgSiH <sub>6</sub>	12 <i>C2/m</i>	250.0	63.144	0.1
237	MgSiH <sub>6</sub>	12 <i>C2/m</i>	275.0	58.048	0.1
238	MgSiH <sub>6</sub>	12 <i>C2/m</i>	300.0	52.651	0.1
239	Li <sub>2</sub> BH <sub>6</sub>	175 <i>P6/m</i>	100.0	98.0	0.1
240	Li <sub>2</sub> BH <sub>6</sub>	175 <i>P6/m</i>	200.0	81.0	0.1
241	VH	166 <i>R<math>\bar{3}</math>m</i>	200.0	2.24	0.1
242	VH <sub>2</sub>	62 <i>Pnma</i>	200.0	6.12	0.1
243	VH <sub>3</sub>	225 <i>Fm<math>\bar{3}</math>m</i>	200.0	4.59	0.1
244	VH <sub>5</sub>	194 <i>P6<sub>3</sub>/mmm</i>	200.0	18.5	0.1
245	VH <sub>5</sub>	63 <i>Cmcm</i>	300.0	25.1	0.1
246	VH <sub>8</sub>	12 <i>C2/m</i>	300.0	71.4	0.1
247	TaH <sub>2</sub>	62 <i>Pnma</i>	200.0	7.1	0.1
248	TaH <sub>4</sub>	166 <i>R<math>\bar{3}</math>m</i>	250.0	31.0	0.1

249	TaH <sub>6</sub>	43 <i>Fdd2</i>	300.0	135.8	0.1
250	LaH <sub>4</sub>	139 <i>I4/mmm</i>	300.0	10.0	0.1
251	LaH <sub>8</sub>	12 <i>C2/m</i>	300.0	131.0	0.1
252	LaH <sub>10</sub>	225 <i>Fm<math>\bar{3}</math>m</i>	210.0	238.0	0.1
253	LaH <sub>10</sub>	225 <i>Fm<math>\bar{3}</math>m</i>	250.0	232.0	0.1
254	LaH <sub>10</sub>	225 <i>Fm<math>\bar{3}</math>m</i>	300.0	215.0	0.1
255	YH <sub>10</sub>	229 <i>Im<math>\bar{3}</math>m</i>	250.0	265.0	0.1
256	YH <sub>10</sub>	229 <i>Im<math>\bar{3}</math>m</i>	300.0	255.0	0.1
257	H <sub>2</sub> Cl	166 <i>R<math>\bar{3}</math>m</i>	400.0	44.8	0.1
258	ArH	2 <i>P<math>\bar{1}</math></i>	1400.0	6.0	0.1
259	ArH <sub>2</sub>	12 <i>C2/m</i>	1500.0	70.0	0.1
260	ArH <sub>4</sub>	139 <i>I4/mmm</i>	1500.0	72.0	0.1
261	ArH <sub>4</sub>	62 <i>Pnma</i>	2000.0	51.0	0.1
262	ZrH	63 <i>Cmcm</i>	120.0	10.6	0.1
263	ScH <sub>6</sub>	194 <i>P6<sub>3</sub>/mmc</i>	300.0	95.03	0.1
264	ScH <sub>9</sub>	194 <i>P6<sub>3</sub>/mmc</i>	400.0	183.1	0.1
265	YH <sub>6</sub>	229 <i>Im<math>\bar{3}</math>m</i>	120.0	259.6	0.1
266	YH <sub>9</sub>	176 <i>P6<sub>3</sub>/m</i>	150.0	264.2	0.1
267	YH <sub>10</sub>	225 <i>Fm<math>\bar{3}</math>m</i>	400.0	308.3	0.1
268	LaH <sub>6</sub>	166 <i>R<math>\bar{3}</math>m</i>	100.0	231.8	0.1
269	CeH <sub>9</sub>	194 <i>P6<sub>3</sub>/mmc</i>	50.0	60.26	0.1
270	GeH <sub>4</sub>	12 <i>C2/m</i>	280.0	67.0	0.1
271	GeH <sub>4</sub>	12 <i>C2/m</i>	300.0	63.0	0.1
272	Ge <sub>3</sub> H <sub>11</sub>	119 <i>I<math>\bar{4}</math>m2</i>	285.0	43.0	0.1
273	Ge <sub>3</sub> H <sub>11</sub>	119 <i>I<math>\bar{4}</math>m2</i>	300.0	38.0	0.1
274	Ge <sub>3</sub> H <sub>11</sub>	119 <i>I<math>\bar{4}</math>m2</i>	320.0	35.0	0.1
275	FeH <sub>5</sub>	67 <i>Cmma</i>	200.0	48.0	0.1
276	FeH <sub>5</sub>	139 <i>I4/mmm</i>	200.0	0.1	0.1
277	FeH <sub>5</sub>	64 <i>Cmca</i>	300.0	0.1	0.1
278	AcH <sub>3</sub>	63 <i>Cmcm</i>	150.0	0.0	0.1
279	Ac <sub>3</sub> H <sub>10</sub>	65 <i>Cmmm</i>	150.0	3.0	0.1
280	AcH <sub>4</sub>	63 <i>Cmcm</i>	100.0	60.0	0.1
281	AcH <sub>5</sub>	2 <i>P<math>\bar{1}</math></i>	150.0	74.9	0.1
282	AcH <sub>8</sub>	12 <i>C2/m</i>	150.0	134.0	0.1
283	AcH <sub>10</sub>	8 <i>Cm</i>	100.0	152.1	0.1
284	AcH <sub>10</sub>	166 <i>R<math>\bar{3}</math>m</i>	200.0	204.1	0.1
285	AcH <sub>10</sub>	166 <i>R<math>\bar{3}</math>m</i>	250.0	140.1	0.1
286	AcH <sub>10</sub>	166 <i>R<math>\bar{3}</math>m</i>	300.0	83.2	0.1
287	AcH <sub>12</sub>	139 <i>I4/mmm</i>	150.0	123.3	0.1
288	AcH <sub>12</sub>	139 <i>I4/mmm</i>	300.0	83.8	0.1
289	AcH <sub>16</sub>	175 <i>P6/m2</i>	150.0	199.2	0.1
290	AcH <sub>16</sub>	175 <i>P6/m2</i>	250.0	155.9	0.1
291	H <sub>3</sub> SXe	221 <i>Pm<math>\bar{3}</math>m</i>	240.0	89.0	0.13
292	H <sub>3</sub> SAr	221 <i>Pm<math>\bar{3}</math>m</i>	240.0	22.0	0.13
293	ScH <sub>2</sub>	191 <i>P6/mmm</i>	300.0	0.0	0.1
294	ScH <sub>3</sub>	194 <i>P6<sub>3</sub>/mmc</i>	400.0	0.0	0.1
295	ScH <sub>4</sub>	139 <i>I4/mmm</i>	120.0	105.0	0.1
296	ScH <sub>4</sub>	139 <i>I4/mmm</i>	250.0	72.0	0.1
297	ScH <sub>6</sub>	229 <i>Im<math>\bar{3}</math>m</i>	250.0	149.0	0.1
298	ScH <sub>7</sub>	63 <i>Cmcm</i>	300.0	201.0	0.1
299	ScH <sub>9</sub>	109 <i>I4<sub>1</sub>md</i>	300.0	187.0	0.1
300	ScH <sub>10</sub>	63 <i>Cmcm</i>	250.0	129.0	0.1
301	ScH <sub>12</sub>	71 <i>Immm</i>	350.0	155.0	0.1
302	ThH <sub>3</sub>	166 <i>R<math>\bar{3}</math>m</i>	100.0	0.0	0.1
303	Th <sub>3</sub> H <sub>10</sub>	71 <i>Immm</i>	10.0	3.8	0.1
304	ThH <sub>4</sub>	139 <i>I4/mmm</i>	85.0	2.97	0.1
305	ThH <sub>7</sub>	14 <i>P2<sub>1</sub>/c</i>	100.0	61.4	0.1
306	ThH <sub>10</sub>	225 <i>Fm<math>\bar{3}</math>m</i>	100.0	221.1	0.1
307	ThH <sub>10</sub>	225 <i>Fm<math>\bar{3}</math>m</i>	200.0	182.6	0.1
308	ThH <sub>10</sub>	225 <i>Fm<math>\bar{3}</math>m</i>	300.0	155.4	0.1
309	H <sub>3</sub> Cl	229 <i>Im<math>\bar{3}</math>m</i>	150.0	198.0	0.1
310	H <sub>3</sub> Cl	229 <i>Im<math>\bar{3}</math>m</i>	175.0	122.0	0.1
311	H <sub>3</sub> Cl	229 <i>Im<math>\bar{3}</math>m</i>	200.0	95.0	0.1

312	H <sub>3</sub> Cl	229 <i>Im</i> $\bar{3}m$	250.0	77.0	0.1
313	WH	194 <i>P6</i> <sub>3</sub> / <i>mmc</i>	300.0	4.175	0.1
314	WH <sub>2</sub>	62 <i>Pnma</i>	300.0	1.484	0.1
315	WH <sub>4</sub>	129 <i>P4/nmm</i>	140.0	0.065	0.1
316	WH <sub>5</sub>	183 <i>P6mm</i>	230.0	64.16	0.1
317	WH <sub>5</sub>	183 <i>P6mm</i>	250.0	64.87	0.1
318	WH <sub>5</sub>	183 <i>P6mm</i>	270.0	62.41	0.1
319	WH <sub>5</sub>	183 <i>P6mm</i>	300.0	60.792	0.1
320	WH <sub>6</sub>	12 <i>C2/m</i>	240.0	31.586	0.1
321	H <sub>6</sub> SSe	221 <i>Pm</i> $\bar{3}m$	200.0	196.0	0.1
322	H <sub>6</sub> SSe	65 <i>Cmmm</i>	200.0	181.0	0.1
323	H <sub>6</sub> SSe	227 <i>Fd</i> $\bar{3}m$	200.0	115.0	0.1
324	ZrH <sub>3</sub>	161 <i>R3c</i>	260.0	8.0	0.13
325	ZrH <sub>4</sub>	70 <i>Fddd</i>	140.0	78.0	0.13
326	ZrH <sub>4</sub>	139 <i>I4/mmm</i>	230.0	47.0	0.13
327	ZrH <sub>6</sub>	36 <i>Cmc21-HP</i>	160.0	55.0	0.13
328	ZrH <sub>6</sub>	36 <i>Cmc21-HP</i>	215.0	70.0	0.13
329	ZrH <sub>6</sub>	14 <i>P2</i> <sub>1</sub> / <i>c</i>	295.0	153.0	0.13
330	ZrH <sub>6</sub>	139 <i>I4/mmm</i>	295.0	114.0	0.13
331	ZrH <sub>6</sub>	139 <i>I4/mmm</i>	340.0	107.0	0.13
332	H <sub>3</sub> S <sub>0.875</sub> P <sub>0.125</sub>	166 <i>R</i> $\bar{3}m$	100.0	136.0	0.1
333	H <sub>3</sub> S <sub>0.875</sub> P <sub>0.125</sub>	166 <i>R</i> $\bar{3}m$	150.0	168.0	0.1
334	H <sub>3</sub> S <sub>0.875</sub> P <sub>0.125</sub>	229 <i>Im</i> $\bar{3}m$	200.0	194.0	0.1
335	H <sub>3</sub> S <sub>0.875</sub> P <sub>0.125</sub>	229 <i>Im</i> $\bar{3}m$	250.0	178.0	0.1
336	HS <sub>0.9375</sub> P <sub>0.0625</sub>	166 <i>R</i> $\bar{3}m$	100.0	131.3	0.1
337	HS <sub>0.9375</sub> P <sub>0.0625</sub>	166 <i>R</i> $\bar{3}m$	150.0	170.5	0.1
338	HS <sub>0.9375</sub> P <sub>0.0625</sub>	229 <i>Im</i> $\bar{3}m$	200.0	212.3	0.1
339	HS <sub>0.9375</sub> P <sub>0.0625</sub>	229 <i>Im</i> $\bar{3}m$	250.0	190.7	0.1
340	HS <sub>0.9375</sub> P <sub>0.0625</sub>	166 <i>R</i> $\bar{3}m$	100.0	126.7	0.1
341	HS <sub>0.9375</sub> P <sub>0.0625</sub>	166 <i>R</i> $\bar{3}m$	150.0	145.4	0.1
342	HS <sub>0.9375</sub> P <sub>0.0625</sub>	229 <i>Im</i> $\bar{3}m$	200.0	161.4	0.1
343	HS <sub>0.9375</sub> P <sub>0.0625</sub>	229 <i>Im</i> $\bar{3}m$	250.0	142.3	0.1
344	H <sub>3</sub> S <sub>0.875</sub> Cl <sub>0.125</sub>	166 <i>R</i> $\bar{3}m$	100.0	139.5	0.1
345	H <sub>3</sub> S <sub>0.875</sub> Cl <sub>0.125</sub>	166 <i>R</i> $\bar{3}m$	150.0	147.8	0.1
346	H <sub>3</sub> S <sub>0.875</sub> Cl <sub>0.125</sub>	229 <i>Im</i> $\bar{3}m$	200.0	136.1	0.1
347	H <sub>3</sub> S <sub>0.875</sub> Cl <sub>0.125</sub>	229 <i>Im</i> $\bar{3}m$	250.0	119.4	0.1
348	TiH	139 <i>I4/mmm</i>	200.0	11.8	0.1
349	TiH <sub>2</sub>	139 <i>I4/mmm</i>	30.0	0.0	0.1
350	TiH <sub>2</sub>	129 <i>P4/nmm</i>	200.0	0.1	0.1
351	TiH <sub>3</sub>	225 <i>Fm</i> $\bar{3}m$	80.0	13.3	0.1
352	TiH <sub>3</sub>	225 <i>Fm</i> $\bar{3}m$	100.0	9.7	0.1
353	TiH <sub>3</sub>	225 <i>Fm</i> $\bar{3}m$	150.0	5.0	0.1
354	TiH <sub>3</sub>	225 <i>Fm</i> $\bar{3}m$	200.0	3.5	0.1
355	TiH <sub>6</sub>	71 <i>Immm</i>	200.0	77.8	0.1
356	VH <sub>3</sub>	229 <i>Fm</i> $\bar{3}m$	140.0	11.1	0.1
357	VH <sub>3</sub>	229 <i>Fm</i> $\bar{3}m$	150.0	8.0	0.1
358	VH <sub>3</sub>	229 <i>Fm</i> $\bar{3}m$	200.0	2.5	0.1
359	VH <sub>3</sub>	229 <i>Fm</i> $\bar{3}m$	250.0	1.6	0.1
360	PdH	216 <i>F</i> $\bar{4}3m$	200.0	8.86	0.1
361	PdH <sub>2</sub>	225 <i>Fm</i> $\bar{3}m$	200.0	18.78	0.1
362	FeH <sub>5</sub>	139 <i>I4/mmm</i>	150.0	45.8	0.1
363	FeH <sub>5</sub>	139 <i>I4/mmm</i>	300.0	35.7	0.1
364	FeH <sub>6</sub>	12 <i>C2/m</i>	100.0	3.9	0.1
365	FeH <sub>6</sub>	65 <i>Cmmm</i>	150.0	42.9	0.1
366	FeH <sub>6</sub>	65 <i>Cmmm</i>	300.0	37.3	0.1
367	H <sub>6</sub> Se	51 <i>Pnma</i>	150.0	39.0	0.1
368	H <sub>6</sub> Se	51 <i>Pnma</i>	200.0	28.0	0.1
369	H <sub>6</sub> Se	51 <i>Pnma</i>	300.0	26.0	0.1
370	H <sub>6</sub> Se	12 <i>C2/m</i>	265.0	87.0	0.1
371	H <sub>6</sub> Se	12 <i>C2/m</i>	270.0	86.0	0.1
372	H <sub>6</sub> Se	12 <i>C2/m</i>	300.0	56.0	0.1
373	YH <sub>6</sub>	229 <i>Im</i> $\bar{3}m$	100.0	233.0	0.1
374	YH <sub>6</sub>	229 <i>Im</i> $\bar{3}m$	125.0	165.0	0.1

375	YH <sub>6</sub>	229 $Im\bar{3}m$	200.0	285.0	0.1
376	YH <sub>6</sub>	229 $Im\bar{3}m$	300.0	290.0	0.1
377	CaYH <sub>12</sub>	221 $Pm\bar{3}m$	170.0	210.0	0.1
378	CaYH <sub>12</sub>	221 $Pm\bar{3}m$	200.0	215.0	0.1
379	CaYH <sub>12</sub>	221 $Pm\bar{3}m$	250.0	201.0	0.1
380	CaYH <sub>12</sub>	227 $Fd\bar{3}m$	200.0	226.0	0.1
381	MgH <sub>16</sub>	2 $P\bar{1}$	300.0	73.0	0.1
382	LiMgH <sub>16</sub>	1 $P1$	300.0	178.0	0.1
383	Li <sub>2</sub> MgH <sub>16</sub>	156 $P\bar{3}m1$	300.0	201.0	0.1
384	Li <sub>2</sub> MgH <sub>16</sub>	227 $Fd\bar{3}m$	250.0	473.0	0.1
385	Li <sub>2</sub> MgH <sub>16</sub>	227 $Fd\bar{3}m$	300.0	357.0	0.1
386	Li <sub>2</sub> MgH <sub>16</sub>	227 $Fd\bar{3}m$	500.0	176.0	0.1
387	Li <sub>3</sub> MgH <sub>16</sub>	5 $C2$	300.0	212.0	0.1
388	YH <sub>6</sub>	229 $Im\bar{3}m$	250.0	300.0	0.11
389	YH <sub>6</sub>	229 $Im\bar{3}m$	350.0	283.0	0.11
390	YH <sub>10</sub>	225 $Fm\bar{3}m$	250.0	311.0	0.11
391	YH <sub>10</sub>	225 $Fm\bar{3}m$	300.0	310.0	0.11
392	YH <sub>10</sub>	225 $Fm\bar{3}m$	350.0	278.0	0.11
393	YS <sub>4</sub> H <sub>4</sub>	12 $C2/m$	200.0	20.0	0.1
394	FeSeH	12 $C2/m$	150.0	0.2	0.1
395	FeSeH	12 $C2/m$	200.0	0.0	0.1
396	FeSeH	12 $C2/m$	250.0	0.0	0.1
397	FeSeH	12 $C2/m$	300.0	0.0	0.1
398	Fe <sub>2</sub> SeH	71 $Immm$	150.0	1.1	0.1
399	Fe <sub>2</sub> SeH	71 $Immm$	200.0	0.8	0.1
400	Fe <sub>2</sub> SeH	71 $Immm$	250.0	3.8	0.1
401	Fe <sub>2</sub> SeH	71 $Immm$	300.0	1.3	0.1
402	Fe <sub>2</sub> SeH <sub>2</sub>	38 $Amm2$	150.0	0.0	0.1
403	Fe <sub>2</sub> SeH <sub>2</sub>	139 $I4/mmm$	150.0	8.6	0.1
404	Fe <sub>2</sub> SeH <sub>2</sub>	139 $I4/mmm$	200.0	9.1	0.1
405	FeSeH <sub>6</sub>	6 $Pm$	150.0	34.4	0.1
406	FeSeH <sub>6</sub>	6 $Pm$	200.0	36.4	0.1
407	Fe <sub>2</sub> SeH <sub>6</sub>	47 $Pmmm$	150.0	0.0	0.1
408	CeH <sub>9</sub>	216 $F\bar{4}3m$	90.0	133.811	0.1
409	CeH <sub>9</sub>	216 $F\bar{4}3m$	92.0	141.691	0.1
410	CeH <sub>9</sub>	216 $F\bar{4}3m$	94.0	142.558	0.1
411	CeH <sub>9</sub>	216 $F\bar{4}3m$	96.0	116.405	0.1
412	CeH <sub>9</sub>	216 $F\bar{4}3m$	98.0	140.482	0.1
413	CeH <sub>9</sub>	216 $F\bar{4}3m$	100.0	141.236	0.1
414	CeH <sub>9</sub>	216 $F\bar{4}3m$	150.0	130.651	0.1
415	CeH <sub>9</sub>	216 $F\bar{4}3m$	200.0	113.98	0.1
416	CeH <sub>9</sub>	216 $F\bar{4}3m$	250.0	97.608	0.1
417	CeH <sub>9</sub>	216 $F\bar{4}3m$	300.0	93.647	0.1
418	CeH <sub>10</sub>	225 $Fm\bar{3}m$	92.0	147.143	0.1
419	CeH <sub>10</sub>	225 $Fm\bar{3}m$	94.0	168.133	0.1
420	CeH <sub>10</sub>	225 $Fm\bar{3}m$	96.0	117.656	0.1
421	CeH <sub>10</sub>	225 $Fm\bar{3}m$	98.0	125.005	0.1
422	CeH <sub>10</sub>	225 $Fm\bar{3}m$	100.0	144.022	0.1
423	CeH <sub>10</sub>	225 $Fm\bar{3}m$	150.0	134.382	0.1
424	CeH <sub>10</sub>	225 $Fm\bar{3}m$	200.0	105.745	0.1
425	CeH <sub>10</sub>	225 $Fm\bar{3}m$	250.0	84.766	0.1
426	CeH <sub>10</sub>	225 $Fm\bar{3}m$	300.0	74.129	0.1
427	LiPH <sub>3</sub>	10 $P2/m$	200.0	60.4	0.1
428	LiPH <sub>4</sub>	11 $P2_1/m$	150.0	0.05	0.1
429	LiPH <sub>6</sub>	200 $Pm\bar{3}$	200.0	167.3	0.1
430	LiPH <sub>6</sub>	200 $Pm\bar{3}$	250.0	148.3	0.1
431	LiPH <sub>6</sub>	200 $Pm\bar{3}$	300.0	128.6	0.1
432	LiPH <sub>7</sub>	12 $C2/m$	300.0	59.2	0.1
433	YCaH <sub>12</sub>	221 $Pm\bar{3}m$	180.0	229.9	0.1
434	YCaH <sub>12</sub>	221 $Pm\bar{3}m$	200.0	222.0	0.1
435	YCaH <sub>12</sub>	221 $Pm\bar{3}m$	250.0	210.8	0.1
436	YSH <sub>6</sub>	131 $P4_2/mmc$	210.0	91.0	0.1
437	YSH <sub>6</sub>	131 $P4_2/mmc$	300.0	61.0	0.1

438	LaSH <sub>6</sub>	63 <i>Cmcm</i>	200.0	24.0	0.1
439	LaSH <sub>6</sub>	63 <i>Cmcm</i>	300.0	35.0	0.1
440	PH <sub>3</sub>	63 <i>Cmcm</i>	100.0	13.0	0.13
441	PH <sub>3</sub>	12 <i>C2/m</i>	200.0	67.0	0.13
442	UH <sub>10</sub>	225 <i>Fm<math>\bar{3}</math>m</i>	100.0	58.58	0.1
443	UH <sub>10</sub>	225 <i>Fm<math>\bar{3}</math>m</i>	200.0	21.22	0.1
444	UH <sub>10</sub>	225 <i>Fm<math>\bar{3}</math>m</i>	300.0	11.93	0.1
445	UH <sub>10</sub>	225 <i>Fm<math>\bar{3}</math>m</i>	400.0	9.5	0.1
446	UH <sub>10</sub>	225 <i>Fm<math>\bar{3}</math>m</i>	550.0	15.11	0.1
447	S <sub>0.2</sub> Se <sub>0.8</sub> H <sub>3</sub>	166 <i>R<math>\bar{3}</math>m</i>	200.0	110.0	0.1
448	S <sub>0.3</sub> Se <sub>0.6</sub> H <sub>3</sub>	156 <i>P<math>\bar{3}</math>m1</i>	200.0	54.0	0.1
449	S <sub>0.5</sub> Se <sub>0.5</sub> H <sub>3</sub>	166 <i>R<math>\bar{3}</math>m</i>	200.0	99.0	0.1
450	S <sub>0.6</sub> Se <sub>0.4</sub> H <sub>3</sub>	166 <i>R<math>\bar{3}</math>m</i>	200.0	184.0	0.1
451	TaH <sub>5</sub>	14 <i>P2<sub>1</sub>/c</i>	100.0	23.0	0.1
452	BH <sub>2</sub>	15 <i>C2/c</i>	250.0	37.31	0.1
453	BH <sub>2</sub>	15 <i>C2/c</i>	300.0	34.24	0.1
454	BH <sub>2</sub>	15 <i>C2/c</i>	350.0	33.31	0.1
455	BH <sub>2</sub>	15 <i>C2/c</i>	400.0	28.03	0.1
456	BH	191 <i>P6/mmm</i>	250.0	4.522	0.1
457	NiH <sub>2</sub>	225 <i>Fm<math>\bar{3}</math>m</i>	25.0	0.01	0.1
458	Al <sub>2</sub> H	156 <i>P<math>\bar{3}</math>m1</i>	195.0	3.5	0.13
459	Al <sub>2</sub> H	148 <i>R<math>\bar{3}</math></i>	195.0	0.6	0.13
460	Al <sub>2</sub> H	150 <i>P321</i>	195.0	0.6	0.13
461	Al <sub>2</sub> H	10 <i>P2/m</i>	195.0	1.2	0.13
462	Al <sub>2</sub> H	5 <i>C2</i>	195.0	0.4	0.13
463	AlH	166 <i>R<math>\bar{3}</math>m</i>	180.0	57.9	0.13
464	AlH	166 <i>R<math>\bar{3}</math>m</i>	215.0	45.4	0.13
465	AlH	166 <i>R<math>\bar{3}</math>m</i>	335.0	21.2	0.13
466	AlH <sub>3</sub>	223 <i>Pm<math>\bar{3}</math>n</i>	105.0	28.5	0.13
467	AlH <sub>3</sub>	223 <i>Pm<math>\bar{3}</math>n</i>	150.0	7.7	0.13
468	AlH <sub>3</sub>	223 <i>Pm<math>\bar{3}</math>n</i>	210.0	0.3	0.13
469	AlH <sub>3</sub>	223 <i>Pm<math>\bar{3}</math>n</i>	290.0	0.0	0.13
470	HBS	40 <i>Ama2</i>	200.0	0.0	0.1
471	HBS	40 <i>Ama2</i>	300.0	0.8	0.1
472	HBS	40 <i>Ama2</i>	400.0	1.9	0.1
473	CaB <sub>3</sub> H	38 <i>Amm2</i>	300.0	7.0	0.1
474	CaBH	46 <i>Ima2</i>	300.0	0.1	0.1
475	CaBH <sub>5</sub>	194 <i>P6mmc</i>	300.0	0.1	0.1
476	CaBH <sub>6</sub>	205 <i>Pa<math>\bar{3}</math></i>	100.0	114.0	0.1
477	CaBH <sub>6</sub>	205 <i>Pa<math>\bar{3}</math></i>	200.0	117.0	0.1
478	CaBH <sub>6</sub>	205 <i>Pa<math>\bar{3}</math></i>	300.0	119.0	0.1
479	Ca <sub>2</sub> B <sub>2</sub> H <sub>13</sub>	6 <i>Pm</i>	200.0	63.0	0.1
480	Ca <sub>2</sub> B <sub>2</sub> H <sub>13</sub>	6 <i>Pm</i>	300.0	89.0	0.1
481	TiPH	156 <i>P3m1</i>	150.0	0.0	0.1
482	TiPH <sub>2</sub>	166 <i>R<math>\bar{3}</math>m</i>	250.0	2.22	0.1
483	TiPH <sub>3</sub>	38 <i>Amm2</i>	250.0	30.51	0.1
484	TiPH <sub>4</sub>	166 <i>R<math>\bar{3}</math>m</i>	100.0	51.57	0.1
485	TiPH <sub>4</sub>	166 <i>R<math>\bar{3}</math>m</i>	200.0	38.09	0.1
486	TiPH <sub>4</sub>	166 <i>R<math>\bar{3}</math>m</i>	250.0	62.36	0.1
487	TiPH <sub>4</sub>	166 <i>R<math>\bar{3}</math>m</i>	300.0	57.06	0.1
488	TiPH <sub>5</sub>	119 <i>I4m2</i>	250.0	126.06	0.1
489	TiPH <sub>6</sub>	8 <i>Cm</i>	250.0	40.89	0.1
490	TiPH <sub>7</sub>	8 <i>Cm</i>	250.0	51.32	0.1
491	TiPH <sub>8</sub>	12 <i>C2/m</i>	250.0	66.67	0.1
492	TiPH <sub>8</sub>	12 <i>C2/m</i>	300.0	54.77	0.1
493	BeCH <sub>4</sub>	2 <i>P<math>\bar{1}</math></i>	5.0	6.0	0.1
494	BeCH <sub>4</sub>	2 <i>P<math>\bar{1}</math></i>	60.0	8.5	0.1
495	BeCH <sub>4</sub>	2 <i><math>\beta</math>-P<math>\bar{1}</math></i>	20.0	13.3	0.1
496	BeCH <sub>4</sub>	2 <i><math>\alpha</math>-P<math>\bar{1}</math></i>	40.0	18.1	0.1
497	BeCH <sub>4</sub>	2 <i><math>\alpha</math>-P<math>\bar{1}</math></i>	80.0	28.9	0.1
498	Zr <sub>4</sub> H <sub>15</sub>	220 <i>I43d</i>	40.0	0.8	0.1
499	ZrH <sub>3</sub>	223 <i>Pm<math>\bar{3}</math>n</i>	10.0	16.6	0.1
500	ZrH <sub>3</sub>	223 <i>Pm<math>\bar{3}</math>n</i>	20.0	13.8	0.1

501	ZrH <sub>3</sub>	223 <i>Pm</i> $\bar{3}n$	40.0	12.4	0.1
502	TiH <sub>22</sub>	12 <i>C2/m</i>	350.0	93.6	0.1
503	TiH <sub>22</sub>	12 <i>C2/m</i>	250.0	103.1	0.1
504	TiH <sub>14</sub>	12 <i>C2/m</i>	200.0	35.0	0.1
505	TiH <sub>12</sub>	2 <i>P</i> $\bar{1}$	350.0	18.8	0.1
506	TiH <sub>12</sub>	2 <i>P</i> $\bar{1}$	150.0	4.8	0.1
507	Ti <sub>2</sub> H <sub>13</sub>	71 <i>Immm</i>	350.0	131.2	0.1
508	TiH <sub>4</sub>	70 <i>Fddd</i>	350.0	21.2	0.1
509	Ti <sub>5</sub> H <sub>14</sub>	82 <i>I</i> $\bar{4}$	350.0	2.4	0.1
510	Ti <sub>5</sub> H <sub>14</sub>	82 <i>I</i> $\bar{4}$	50.0	5.4	0.1
511	Ti <sub>5</sub> H <sub>13</sub>	87 <i>I4/m</i>	300.0	4.0	0.1
512	Ti <sub>5</sub> H <sub>13</sub>	87 <i>I4/m</i>	150.0	2.1	0.1
513	Ti <sub>2</sub> H <sub>5</sub>	72 <i>Ibam</i>	250.0	4.7	0.1
514	Ti <sub>2</sub> H <sub>5</sub>	72 <i>Ibam</i>	50.0	7.1	0.1
515	TiH <sub>2</sub>	67 <i>Cmma</i>	250.0	5.8	0.1
516	TiH <sub>2</sub>	139 <i>I4/mmm</i>	50.0	0.0	0.1
517	TiH	166 <i>R</i> $\bar{3}m$	350.0	22.7	0.1
518	TiH	139 <i>I4/mmm</i>	50.0	5.4	0.1
519	LiP <sub>2</sub> H <sub>14</sub>	148 <i>R</i> $\bar{3}$	230.0	143.0	0.1
520	LiP <sub>2</sub> H <sub>14</sub>	148 <i>R</i> $\bar{3}$	300.0	112.0	0.1
521	LiP <sub>2</sub> H <sub>14</sub>	148 <i>R</i> $\bar{3}$	400.0	84.0	0.1
522	BeP <sub>2</sub> H <sub>14</sub>	148 <i>R</i> $\bar{3}$	400.0	90.0	0.1
523	NaP <sub>2</sub> H <sub>14</sub>	148 <i>R</i> $\bar{3}$	400.0	139.0	0.1
524	LiBH <sub>2</sub>	63 <i>cmcm</i>	300.0	0.99	0.1
525	LiBH <sub>2</sub>	63 <i>cmcm</i>	400.0	2.33	0.1
526	LiBH <sub>2</sub>	63 <i>cmcm</i>	500.0	9.12	0.1
527	LiBH <sub>2</sub>	63 <i>cmcm</i>	600.0	10.0	0.1
528	CSH <sub>7</sub>	8 <i>Cm</i>	100.0	98.0	0.1
529	CSH <sub>7</sub>	166 <i>R</i> $\bar{3}m$	150.0	152.0	0.1
530	CSH <sub>7</sub>	166 <i>R</i> $\bar{3}m$	200.0	137.0	0.1
531	CSH <sub>7</sub>	53 <i>Pmna</i>	150.0	122.0	0.1
532	CSH <sub>7</sub>	53 <i>Pmna</i>	200.0	123.0	0.1